ORIGINAL RESEARCH

Beneficial Pleiotropic Antidepressive Effects of Cardiovascular Disease Risk Factor Interventions in the Metabolic Syndrome

Stephanie J. Frisbee, PhD, MSc; Sarah S. Singh, MD, MPH; Dwayne N. Jackson, PhD; Kent A. Lemaster, MSc; Samantha A. Milde, MSc; J. Kevin Shoemaker, PhD; Jefferson C. Frisbee, PhD

***Background*—**Although the increased prevalence and severity of clinical depression and elevated cardiovascular disease risk represent 2 vexing public health issues, the growing awareness of their combined presentation compounds the challenge. The obese Zucker rat, a model of the metabolic syndrome, spontaneously develops significant depressive symptoms in parallel with the progression of the metabolic syndrome and, thus, represents a compelling model for study. The primary objective was to assess the impact on both cardiovascular outcomes, specifically vascular structure and function, and depressive symptoms in obese Zucker rats after aggressive treatment for cardiovascular disease risk factors with long-term exercise or targeted pharmacological interventions.

***Methods and Results*—**We chronically treated obese Zucker rats with clinically relevant interventions against cardiovascular disease risk factors to determine impacts on vascular outcomes and depressive symptom severity. While most of the interventions (chronic exercise, anti-hypertensive, the interventions (long-term exercise, antihypertensive, antidyslipidemia, and antidiabetic) were differentially effective at improving vascular outcomes, only those that also resulted in a significant improvement to oxidant stress, inflammation, arachidonic acid metabolism (prostacyclin versus thromboxane A_2), and their associated sequelae were effective at also blunting depressive symptom severity. Using multivariable analyses, discrimination between the effectiveness of treatment groups to maintain behavioral outcomes appeared to be dependent on breaking the cycle of inflammation and oxidant stress, with the associated outcomes of improving endothelial metabolism and both cerebral and peripheral vascular structure and function.

***Conclusions*—**This initial study provides a compelling framework from which to further interrogate the links between cardiovascular disease risk factors and depressive symptoms and suggests mechanistic links and potentially effective avenues for intervention. **(*J Am Heart Assoc*. 2018;7:e008185. DOI: 10.1161/JAHA.117.008185.)**

Key Words: depression • metabolic syndrome • peripheral vascular disease

The growing prevalence of metabolic diseases presents a consistent threat to cardiovascular health outcomes across many societies.[1–3] The metabolic syndrome is broadly defined as the combined presentation of obesity, impaired glycemic control, atherogenic dyslipidemia, and hypertension, with the additional contributing conditions of pro-oxidant, prothrombotic, and proinflammatory phenotypes.[4] This concomitant constellation of pathological conditions represents a powerful detrimental influence on morbidity and mortality,[5] with enormous impacts on the economic, social, and individual burdens that must be borne as a result.[6,7]

The obese Zucker rat (OZR; *fa/fa*) is regarded as a good animal model of the metabolic syndrome, with high translational relevance to humans.[8] In OZRs, an autosomal recessive mutation that results in a dysfunctional leptin receptor leads to hyperphagia and subsequent hyperphagia-

From the Departments of Pathology and Laboratory Medicine (S.J.F.), Epidemiology and Biostatistics (S.J.F., S.S.S.), Medical Biophysics (D.N.J., K.A.L., J.C.F.), and Physiology and Pharmacology (S.A.M., J.K.S., J.C.F.), Schulich School of Medicine and Dentistry, and School of Kinesiology, Faculty of Health Sciences (J.K.S.), University of Western Ontario, London, Ontario, Canada.

Accompanying Tables S1 through S11 are available at http://jaha.ahajournals.org/content/7/7/e008185/DC1/embed/inline-supplementary-material-1.pdf

Correspondence to: Stephanie J. Frisbee, PhD, MSc, Department of Pathology and Laboratory Medicine, Schulich School of Medicine and Dentistry, University of Western Ontario, 1151 Richmond St, Dental Sciences Bldg, Room 4041, London, Ontario, Canada N6A 5C1. E-mail: sfrisbee@uwo.ca

Received November 22, 2017; accepted March 1, 2018.

Clinical Perspective

What Is New?

- This animal study, using exercise or single-target pharmacologic interventions and multistage statistical modeling, assessed complex relationships between metabolic disease, cardiovascular disease (CVD) risk factors, vascular outcomes, and depressive symptoms.
- Key observations were the pleiotropic effects on behavioral outcomes from cardiovascular-targeted interventions.
- Pharmacologic interventions were effective in restoring the therapeutic target but were highly variable in addressing other vascular and behavioral outcomes.
- Exercise was most effective in maintaining behavioral outcomes, followed by TEMPOL (4-hydroxy-2,2,6,6-tetramethylpiperidin-1-oxyl), pentoxifylline, and atorvastatin.
- The interventions most effective in achieving optimized results in behavioral outcomes and integrated cardiovascular function (exercise, TEMPOL, atorvastatin, and pentoxifylline) all share anti-inflammatory and antioxidant mechanisms.

What Are the Clinical Implications?

- Results suggest that relationships between metabolic disease, CVD risk factors, vascular outcomes, and depressive symptoms may not work through traditional CVD risk factors alone.
- Rather, it is likely that the causal mechanisms involve antioxidant and anti-inflammatory contributors that maintain endothelial function.
- Results highlight the potential utility of novel use of established therapeutics for CVD risk that may provide significant relief from the devastating impact of chronic depressive symptoms.
- It is anticipated that results from this study will provide translationally relevant insight into the primary prevention of both CVD and clinical depression.

induced obesity. Development of the metabolic syndrome follows, with a pattern of cardiovascular dysfunction highly comparable to that in humans. Also similar to health outcomes in humans, OZRs progressively develop vasculopathy coincident with the metabolic syndrome, which ultimately progresses to overt peripheral vascular disease.[9,10] Notably, OZRs,[11,12] as well as other specific rodent models of the metabolic syndrome,[13,14] spontaneously develop compromised behavioral patterns indicative of chronic stress and increased depressive symptoms, including elevations in circulating cortisol and corticosterone levels.[15] This is particularly intriguing, because the presence of chronic stress and depressive symptoms has been identified as powerful risk factors (RFs) for negative cardiovascular and cerebrovascular health outcomes.[16,17] However, the identification of underlying causal mechanisms and, by extension, appropriate interventional strategies between metabolic disease, depressive symptoms, and poor cardiovascular health outcomes remains elusive.

In humans, the use of selective serotonin/norepinephrine reuptake inhibitors, tricyclic antidepressants, and other pharmacological agents is the standard of care for treatment of clinical depression. In addition, some studies have reported a pleiotropic impact of antidepressive therapies on improving cardiovascular disease (CVD) risk and/or cardiovascular health outcomes.[18–20] Furthermore, the increased risk for depression in patients with established CVD is well documented and is the subject of treatment guidelines from the American Heart Association.[17] What is less well understood is if early aggressive treatment against CVD-RFs, so as to slow or prevent the onset of patent CVD (primary prevention), can also serve as primary prevention against the development of depression.

The primary purpose of the present study was to aggressively treat CVD risk with long-term exercise or targeted pharmacological interventions against specific CVD-RFs to assess the impact on both cardiovascular outcomes, specifically vascular structure and function, and behavioral outcomes, specifically the development of depressive symptoms, in OZRs. The secondary purpose of the present study was to apply more advanced analytical approaches to interrogate potential mechanistic links between metabolic disease, CVD-RFs, biomarker expression profiling, altered vascular structure and function, and depressive symptoms. The present study was designed to test the integrated hypothesis that aggressive treatment against CVD-RFs from a modest level of severity will result in significant improvements to both cardiovascular and behavioral outcomes.

Methods

The materials, reagents, equipment, and supplies used in this study are all available from the indicated commercial sources. Because this remains an ongoing and active area of investigation, the data that support the findings of this study can be made available to other qualified researchers, on reasonable request to the corresponding author, for the sole purpose of replicating the statistical analyses.

Lean Zucker rats (LZRs) and OZRs were divided into intervention groups and chronically treated with clinically relevant interventions against CVD-RFs, according to the treatment protocols described later. Animals were assessed for the following: (1) behavioral outcomes (ie, depressive symptoms); (2) vascular outcomes (ie, function and reactivity in skeletal muscle arterioles, cerebral resistance arteries, and

conduit arteries); (3) vascular outcomes (ie, structure in skeletal muscle and the cerebral cortex); (4) integrated vascular outcomes (ie, skeletal muscle blood perfusion); (5) signaling molecule bioavailability; and (6) CVD-RFs, including systemic biomarkers. These methods, including surgical preparations, are now described in detail. The statistical approach and detailed description of analyses performed are also described herein.

Animals

Male LZRs (Harlan/Envigo, Indianapolis, IN) and OZRs (Harlan/Envigo) were acquired at 6 to 7 weeks of age and were given 1 week of acclimation to the local environment. Unless otherwise stated (later), all animals were fed standard chow and tap water ad libitum for all experiments. All rats were housed in an accredited animal care facility at either West Virginia University or the University of Western Ontario, and all protocols received Institutional Animal Care and Use Committee or Canadian Council on Animal Care approval.

At the time of final use, rats were anesthetized with injections of sodium pentobarbital (50 mg/kg via IP injection), and all rats received tracheal intubation to facilitate maintenance of a patent airway. In all rats, a carotid artery and an external jugular vein were cannulated for determination of arterial pressure and for intravenous infusion of additional substances as necessary (eg, anesthetic and heparin). In addition, an aliquot of mixed venous blood was drawn from the jugular vein cannula for a full profiling of metabolic, endocrine, and inflammatory biomarkers (described later), and each animal received a bolus injection of heparin to temporarily reduce the occurrence of blood coagulation without jeopardizing vascular reactivity (500 IU/kg).

Intervention Groups and Treatment Protocols

At 7 to 8 weeks of age, LZRs and OZRs were placed into 1 of the following 11 groups for the duration of the treatment period (the subsequent 9–10 weeks):

1. Aged control group: LZR and OZR aged control group animals were untreated (neither exercise nor pharmacologic intervention) and fed normal food and water ad libitum.
2. Exercise group: OZR animals in this group underwent a long-term treadmill exercise protocol that consisted of 20 m/min, 5% incline, 60 min/d, and 6 d/wk.
3. Antihypertensive treatment groups:
   a. OZR animals in this group were treated with a captopril (angiotensin-converting enzyme inhibitor) at the dose of 60 mg/kg per day mixed in drinking water.
   b. OZR animals in this group were treated with hydralazine (systemic vasodilator) at the dose of 50 mg/kg per day mixed in drinking water.
4. Antidiabetic treatment groups:
   a. OZR animals in this group were treated with metformin (hepatic gluconeogenesis inhibitor) at the dose of 300 mg/kg per day mixed in drinking water.
   b. OZR animals in this group were treated with rosiglitazone (insulin-sensitizing agent) at the dose of 10 mg/kg per day mixed with food.
5. Antidyslipidemia treatment groups:
   a. OZR animals in this group were treated with atorvastatin (HMG Co-A [3-hydroxy-3-methyl-glutaryl-coenzyme A reductase] reductase inhibitor) at the dose of 25 mg/kg per day mixed with food.
   b. OZR animals in this group were treated with gemfibrozil (peroxisome proliferator-activated receptor-α activator) at the dose of 100 mg/kg per day mixed with food.
6. Antioxidant/anti-inflammatory treatment groups:
   a. OZR animals in this group were treated with TEMPOL (antioxidant) at the dose of 10^{-3} mol/L mixed in drinking water.
   b. OZR animals in this group were treated with pentoxifylline (anti-inflammation treatment via tumor necrosis factor [TNF]-α production inhibition) at the dose of 30 mg/kg per day by IP injection.

The dose for each pharmacologic intervention was determined on the basis of the established clinically effective dose for that drug. To maintain the same dose throughout the treatment period, the amount of drug administered was adjusted on a weekly basis to account for changing body weight and food consumption. Each treatment group also included untreated LZRs and OZRs as within-group matched controls (untreated healthy animals and untreated diseased animals). For animals in the aged time control group, assessments and measurements were performed at both 7 weeks old (7W) and 17 weeks old (17W), whereas for animals in all other treatment groups, all assessments and measurements were performed at the conclusion of the treatment period (17W) only. Separate animals were required for ex vivo and in vivo experimental procedures (described later). For final statistical analyses, there were n=8 observations in each animal group within each treatment group (untreated controls and treated OZRs).

Behavioral Outcomes: Depressive Symptoms

In this study, depressive symptoms (both their presence and severity) were assessed by assigning a score to 3 self-care

behaviors: coat status score, grooming latency after a sucrose spray test, and grooming frequency after a sucrose spray test.

Selection of self-care behaviors as an assessment of depressive symptoms in animal behavioral models of depression

Behaviorally based outcome measures are widely used in rodent models of depression, particularly behavioral models of depression (in contrast to genetic animal models of depression), such as those based on chronic mild stress (CMS). The CMS model, and closely related unpredictable CMS model, uses a variety of environmental stressors, such as noise, wet bedding, and alterations to light cycles, to create stress and induce depressive symptoms consistent with human depression. The CMS/unpredictable CMS model has been applied for >30 years, and its validity and reliability in both mice and rats have been widely reviewed and accepted,[21–24] as has the translational relevance of this animal model of depression.[24]

In rodents, behaviorally based outcome measures that quantify depressive symptoms include, most commonly, tail suspension tests, forced exercise tests (swim or treadmill), food or sugar consumption and preference, and self-care behaviors (grooming) in response to a splash test.[25,26] These behavioral assessments, including, and of particular relevance to this study, self-care and grooming behaviors, have been used extensively, by many groups, in both mice and rats,[25,27–32] and have also been used previously by this research team.[11,33,34]

For reasons of scientific rigor, validity, and feasibility, in this study we quantified depressive symptoms using 3 self-care behaviors. Tail suspension tests are not viable in obese rats, such as the OZRs. Furthermore, in this study in which exercise was a distinct treatment group, exercise-based behavioral assessments would introduce substantial bias and confound the interpretation of results. Similarly, direct food or sugar-based assessments are not appropriate and would also likely introduce bias in a hyperphagic animal model of obesity, in which the underlying chronic and profound hyperphagia would likely be the overriding behavioral response. Thus, 3 self-care behaviors (coat status and grooming frequency and latency after a sucrose spray test) were selected as the behavioral outcome measures for this study. The selection of these 3 self-care behaviors is further supported by a recently reported survey of researchers who use behavioral outcome measures in CMS/unpredictable CMS models, which reports the use of these grooming-based behavioral outcome measures in a wide variety of laboratories.[25] Finally, to quantitatively and physiologically support the validity of the 3 self-care behaviors selected for this study, Table S1 reports the correlations between cortisol, a widely used biomarker recognized for its association with both stress and depression,[35,36] and coat status score, grooming frequency, and grooming latency, all of which are statistically significant ($P<0.0001$) and moderately strong (Pearson's correlation coefficient $0.5<\rho<0.7$).

Quantification of depressive symptoms using self-care behaviors

Coat status score, grooming frequency, and grooming latency were determined as follows:

Coat status score: This evaluation addresses long-term grooming behavior. A research assistant completed a visual inspection of the animal before use and evaluated the coat status of the animals. A total cumulative score was computed by giving points of 0 (clean) or 1 (dirty) to 8 body parts (head, neck, dorsal coat, ventral coat, tail, forelimb, hind limb, and genital region). Points were then summed to obtain a total score. A higher coat status score reflects failure to groom and greater depressive symptoms. *Grooming frequency and grooming latency after sucrose spray test:* This test was used to evaluate short-term grooming behavior, defined as cleaning of the fur by licking or scratching. A 10% sucrose solution was sprayed on the dorsal coat of each rat, and grooming activity was recorded for 5 minutes. Because the viscosity of the sucrose solution dirties the coat and induces grooming behavior, depressive symptoms are characterized by an increased grooming latency (idle time between spray and initiation of grooming, recorded in seconds) and decreased grooming frequency (duration of total grooming during the 5-minute period, recorded in seconds).

Vascular Outcomes: Function and Reactivity

In this study, vascular function, specifically vascular reactivity, was assessed in skeletal muscle arterioles, cerebral resistance arteries, and conduit arteries. Ex vivo surgical preparations were used to dissect vessels.

Ex vivo surgical preparation for skeletal muscle arterioles (gracilis arterioles)

After the initial surgery, an incision was made into the medial upper hind limb, and the extraparenchymal resistance artery/first-order arteriole supplying the gracilis muscle was identified. This vessel was cleared of all surrounding tissue along its length and into the gracilis muscle. Subsequently, the section of the vessel that was fully within the gracilis muscle was removed and doubly cannulated on glass micropipettes using a previously well-established procedure.[37] At this point, hind limb conduit arteries were removed from the rat (eg, femoral, popliteal, and saphenous), cleaned, and placed in cold physiologic salt solution (PSS) for subsequent determination of specific signaling metabolites relevant for vascular reactivity (see Signaling Molecule Bioavailability section).

Gastrocnemius muscles (GSN-Ms) from each animal were removed, washed in PSS, and placed in 0.25% formalin for subsequent determination of microvessel density (MVD; see Vascular Outcomes: Structure section).

Ex vivo surgical preparation for cerebral resistance arteries (middle cerebral artery)

While deeply anesthetized, each rat was decapitated and the brain was removed from the skull case and placed in cold PSS (4°C). Subsequently, a middle cerebral artery (MCA) was dissected from its origin at the Circle of Willis, and the remainder of the brain was frozen in optimum cutting temperature compound (OCT; Tissue-Tek® O.C.T., VWR International, Radnor, Pennsylvania) for subsequent determination of cortical MVD (see Vascular Outcomes: Structure section). Each MCA was doubly cannulated, as described previously.[37]

Ex vivo surgical preparation for conduit arteries (descending aorta)

Within each animal, the descending aorta was surgically removed, cleaned of extra connective tissue, and sectioned into rings for ex vivo study using a standard tissue myograph technique.[38]

Determination of vascular reactivity

For both gracilis arterioles (GAs) and MCAs, vessels were placed in a heated chamber (37°C) that allowed the lumen and exterior of the vessel to be perfused and superfused, respectively, with PSS equilibrated with 21% O_2, 5% CO_2, 74% N_2 from separate reservoirs. Vessels were cannulated at both ends with glass micropipettes and were tied (10-0 nylon suture) to the inflow and outflow pipettes, which were connected to a reservoir perfusion system that allowed intraluminal pressure and gas concentrations to be controlled. Any side branches were ligated using a single strand teased from 6 to 0 suture. Vessel diameter was measured using television microscopy and an on-screen video micrometer. Arteries were extended to their in situ length and were equilibrated at 80% of the animal's mean arterial pressure. Active tone for pressurized GA and MCA, calculated as $(\Delta D/D_{max}) \times 100$, where ΔD is the diameter increase from rest in response to Ca^{2+}-free PSS, and D_{max} is the maximum diameter measured at the equilibration pressure in Ca^{2+}-free PSS, averaged 30±3% in LZRs and 32±4% in OZRs for GA and 33±3% in LZRs and 35±4% in OZRs for MCA.

The reactivity of isolated arteries was assessed in response to increasing concentrations of acetylcholine (10^{-10}–10^{-6} mol/L), phenylephrine (for GA only; 10^{-10}–10^{-7} mol/L), and serotonin (for MCA only; 10^{-10}–10^{-7} mol/L), and in response to progressive elevations in intraluminal pressure (myogenic activation; from 0 to 160 mm Hg in randomized 20–mm Hg increments).

At the conclusion of all procedures previously described, in both the GA and MCA, the PSS was replaced with a Ca^{2+}-free PSS containing EGTA and EDTA (to chelate calcium ions), and vessels were treated with 10^{-7} mol/L norepinephrine until all active tone was lost. At that point, vascular diameter (inner and outer wall) changes in response to elevated intraluminal pressure over the 0– to 160–mm Hg range was determined. These data were used for the calculation of vascular stiffness (see Vascular Outcomes: Structure section).

In descending aortic rings, each ring was mounted in a myobath chamber between a fixed point and a force transducer (World Precision Instruments, Sarasota, FL) and set to 0.5 g tension for 45 minutes to equilibrate. The organ baths contained PSS at 37°C aerated with 95% O_2 and 5% CO_2. Rings were preconditioned by treatment with 10^{-7} mol/L phenylephrine for 5 minutes, at which time 10^{-5} mol/L methacholine was added to the bath to assess endothelial integrity. Any ring that failed to demonstrate both a brisk constrictor response to phenylephrine and viable endothelial function was discarded. Subsequently, rings were challenged with increasing concentrations of phenylephrine (10^{-12}–10^{-5} mol/L) or were pretreated with 10^{-7} mol/L phenylephrine and exposed to increasing concentrations of methacholine (10^{-10}–10^{-3} mol/L).

The mechanical responses of ex vivo microvessels or aortic rings after agonist challenge were fit with the 3-parameter logistic equation:

$$y = \min + \left[\frac{\max - \min}{1 + 10^{\log ED_{50} - x}}\right] \quad (1)$$

where y represents the change in arteriolar diameter, "min" and "max" represent the lower and upper bounds, respectively, of the change in diameter or tension with increasing agonist concentration, x is the logarithm of the agonist concentration, and log ED_{50} represents the logarithm of the agonist concentration (x) at which the response (y) is halfway between the lower and upper bounds.

Vascular Outcomes: Structure

In this study, vascular structure, specifically MVD in the skeletal muscle and cerebral cortex and vascular stiffness (stress-strain β) in the GA and MCA, was assessed. Ex vivo surgical preparations were used to isolate tissue beds.

Ex vivo surgical and tissue preparation

In all animals, determination of cerebral cortical and skeletal muscle MVD followed similar procedures. After removal of the MCAs from the Circle of Willis on the base of the brain, the brain was placed in OCT compound (Tissue-Tek® O.C.T., VWR International, Radnor, Pennsylvania) and frozen. Brains were then sliced into 5-μm cross-sections and were then stained

using the established approach developed by Munzenmaier and Greene[39] using primary anti–CD-31 antibody. In contrast, GSN-Ms were embedded in paraffin and cut into 5-μm cross-sections, which were stained with *Griffonia simplicifolia* I lectin (Sigma-Alrich Corp, St Louis, MO), as described previously.[40] This procedure selectively stains all microvessels with a diameter ≤20 μm, preferentially arterioles and capillaries versus venules, regardless of perfusion status.[40]

Determination of MVD

Under microscopy, localization of labeled microvessels was performed with a Nikon E600 upright microscope with a ×20 objective lens. The microscope was coupled to cooled charge-coupled device camera (Micromax; Princeton Instruments Inc, Trenton, NJ). Five nearby 1-mm^2 images were taken from each of 3 sections in the frontal cortex of each brain or in the GSN-Ms, and the mean MVD within these images was taken to represent cortical or skeletal muscle MVD in that animal. All acquired images from individual sections were analyzed for number of microvessels using MetaMorph Imaging software (Universal Imaging Co, Downingtown, PA) or Nikon Elements software.[41]

Mathematical calculation of vascular stiffness

The determination of vascular stiffness, defined as passive arteriolar wall mechanics (indicative of structural alterations to the individual microvessel) and quantified as stress-strain β, was based on those used previously,[42] with minor modification, in both the GA and MCA (surgical preparation and dissection described in Determination of Vascular Reactivity subsection of the Vascular Outcomes: Function and Reactivity section). For the calculation of circumferential stress, intraluminal pressure was converted from mm Hg to N/m^2, where 1 mm Hg=1.334×10^2 N/m^2. Circumferential stress (σ) was then calculated as follows:

$$\sigma = (P_{IL} \times ID)/(2WT) \quad (2)$$

where ID represents arteriolar inner diameter (μm), and WT represents wall thickness (μm) at that intraluminal pressure (P_{IL}).

Circumferential strain (ε) was calculated as follows:

$$\varepsilon = (ID - ID_5)/(ID_5) \quad (3)$$

where ID_5 represents the internal arteriolar diameter at the lowest intraluminal pressure (ie, 5 mm Hg).

The stress versus strain relationship from each vessel was fit (ordinary least squares analyses, r^2>0.85) with the following exponential equation:

$$\sigma = \sigma_5 e^{\beta\varepsilon} \quad (4)$$

where σ_5 represents circumferential stress at ID_5, and β is the slope coefficient describing arterial stiffness.

Higher levels of β are indicative of increasing arterial stiffness (ie, requiring a greater degree of distending pressure to achieve a given level of wall deformation).

Integrated Vascular Outcomes: Skeletal Muscle Blood Perfusion

In this study, integrated vascular outcomes, specifically resting blood flow and blood flow hyperemia in the GSN-Ms, was assessed. In vivo surgical preparations were used to isolate the muscle group.

Surgical preparation of in situ blood-perfused skeletal muscle

In all LZRs and OZRs, the left GSN-M was isolated in situ.[43] Briefly, the left leg received a medial incision from the calcaneus to the femoral triangle, and all muscles, vessels, and connective tissue overlaying the muscle were removed, thus exposing the GSN-M, its vascular supply, and the sciatic nerve. The nerve was isolated and used for initiating muscle contraction via a stimulating electrode attached to an electrical stimulator (Grass SD9; Grass Instruments, Astro-Med, Inc, West Warwick, RI). Branches from the femoral artery that did not perfuse the GSN-Ms directly were ligated or cauterized, depending on size and location. A microcirculation flow probe (Transonic Systems Inc, Ithaca, NY) was placed around the femoral artery, immediately distal to its origin from the iliac artery, to measure blood flow to the GSN-Ms. The entire preparation was covered in PSS-soaked gauze and plastic film to minimize evaporative water loss and was placed under a lamp to maintain temperature at 37°C. At this time, heparin (500 U/kg) was infused via the jugular vein to prevent blood coagulation.

Determination of muscle blood flow parameters

After restoration of baseline conditions, the GSN-M was stimulated to perform (via the sciatic nerve) bouts of isometric twitch contractions (3 Hz, 0.4-ms duration, 5 V) for 3 minutes, with arterial pressure and femoral artery blood flow continuously monitored. GSN-M perfusion and performance data after 3 minutes of contraction were normalized to GSN-M mass, which was not different between LZRs (2.16±0.07 g) and OZRs (2.09±0.10 g).

Signaling Molecule Bioavailability

All harvested conduit arteries from each rat were lightly sectioned into segments of ≈1 mm in length and placed in a chamber for study, superfused with warmed (37°C) PSS equilibrated with 95% O_2 and 5% CO_2. Vascular NO production was assessed using amperometric sensors. An NO sensor (ISO-NOPF 100; World Precision Instruments) was inserted

into the chamber, and a baseline level of current was obtained. Subsequently, increasing concentrations of methacholine (10^{-10}–10^{-6} mol/L) were added to the bath, and the changes in current were determined.

In a separate group of arteries, vascular production of 6-keto-prostaglandin $F_{1\alpha}$ (the stable breakdown product of prostacyclin)[44] and 11-dehydro-thromboxane B_2 (the stable plasma breakdown product of thromboxane A_2 [TxA_2])[45,46] was determined in response to challenge with arachidonic acid (10^{-5} mol/L). Pooled sectioned arteries were left untreated resting in 1.5 mL PSS for 30 minutes under control conditions, after which time the superfusate was removed, snap frozen in liquid N_2, and stored for later analysis. The PSS was replaced with 1.5 mL of a solution of PSS+10^{-5} mol/L arachidonic acid and incubated for an additional 30 minutes, after which time this superfusate was also removed, snap frozen in liquid N_2, and stored for later analysis. Vessel weights were determined after blotting on gauze to remove excess liquid, and metabolite release by the vessels was determined using commercially available enzyme immunoassay kits for 6-keto-prostaglandin $F_{1\alpha}$ and 11-dehydro-thromboxane B_2 (Cayman Chemical, Ann Arbor, MI).

Vascular NO bioavailability measurements were fit with a linear regression equation:

$$y = \alpha_0 + \beta_1 x \quad (5)$$

where y represents the NO concentration, α_0 represents an intercept term, β_1 represents the slope of the relationship, and x represents the log molar concentration of methacholine.

CVD Risk Factors

Blood pressure was determined via a transducer attached to a carotid artery cannula. Using blood drawn from a venous cannula, insulin, cortisol, TNF-α, and nitrotyrosine were measured using commercially available ELISA kits, cholesterol was quantified (Wako Diagnostics, Richmond, VA), and glucose was measured directly via a glucometer (Freestyle; Abbott Diabetes Care, Alameda, CA).

Mathematical and Statistical Analysis

The effectiveness of the long-term interventions at improving specific biological outcomes (eg, biomarkers, vascular outcomes, and behavioral scores) was calculated as follows:

$$\left[\frac{\text{ABS}\left(\text{OZR}_{\text{Treated}} - \overline{\text{OZR}_{\text{UntreatedControlGrp}}}\right)}{\text{ABS}\left(\overline{\text{OZR}_{\text{UntreatedControlGrp}}} - \overline{\text{LZR}_{\text{UntreatedControlGrp}}}\right)}\right] \times 100 \quad (6)$$

where $\overline{\text{LZR}_{\text{UntreatedControlGrp}}}$ and $\overline{\text{OZR}_{\text{UntreatedControlGrp}}}$ represent the mean values of the measured parameter in the untreated within-group control groups, and $\text{OZR}_{\text{Treated}}$ represents the values of the measured parameter as a result of long-term imposition of the given intervention.

Thus, this determines the percentage recovery in a parameter from the control condition in OZRs, back to that in control LZRs, as a result of the specific intervention. These calculations are based on n=8 observations in each animal group within each treatment group (untreated controls and treated OZRs).

Univariate statistical analysis

All data are presented as mean±SE. Statistically significant differences in measured physiological parameters (eg, arterial pressure, blood flow, and MVD), calculated physiological parameters (eg, slope coefficients and upper or lower bounds), and measurements of plasma biomarkers were determined using ANOVA. In all cases, Student-Newman-Keuls post hoc test was used when appropriate, and $P<0.05$ was taken to reflect statistical significance. There was no statistical analysis of data presented in Figures 1 through 5, because there are no a priori reasons to clearly identify what level of recovery is necessarily biologically significant under these conditions or which comparison would be most informative. As such, reference lines at 40% recovery are present in each figure to simply provide an arbitrary context.

Multivariable statistical analysis of results (3 steps)

To interrogate potential mechanistic links between metabolic disease, CVD-RFs, biomarker expression profiling, altered vascular structure and function, and behavioral impairments/depressive symptoms, we used a 3-step advanced multivariable statistical approach.

Step 1: cluster analysis to define behaviorally based outcome groups. K-means cluster analysis was used to guide the assignment of each of the treatment groups to a behaviorally based outcome group. For the cluster analysis, all animals from all 11 treatment groups were included, and the initial cluster analysis was performed without regard to treatment group. Clusters were defined using all 3 behavioral variables (coat status score, grooming latency, and grooming frequency); the F-statistic (ANOVA) for the mean square for each of the 3 variables included in the cluster analysis was statistically significant ($P<0.0001$ for each of the 3 variables). Additional details from this statistical analysis are reported in Tables S2 and S3.

Four clusters were identified and, although there was some within–treatment group heterogeneity for cluster mapping, the final outcome group assignment placed all animals in the treatment group to the cluster, where most of the animals in that group mapped. The 4 final outcome groups were defined as follows:

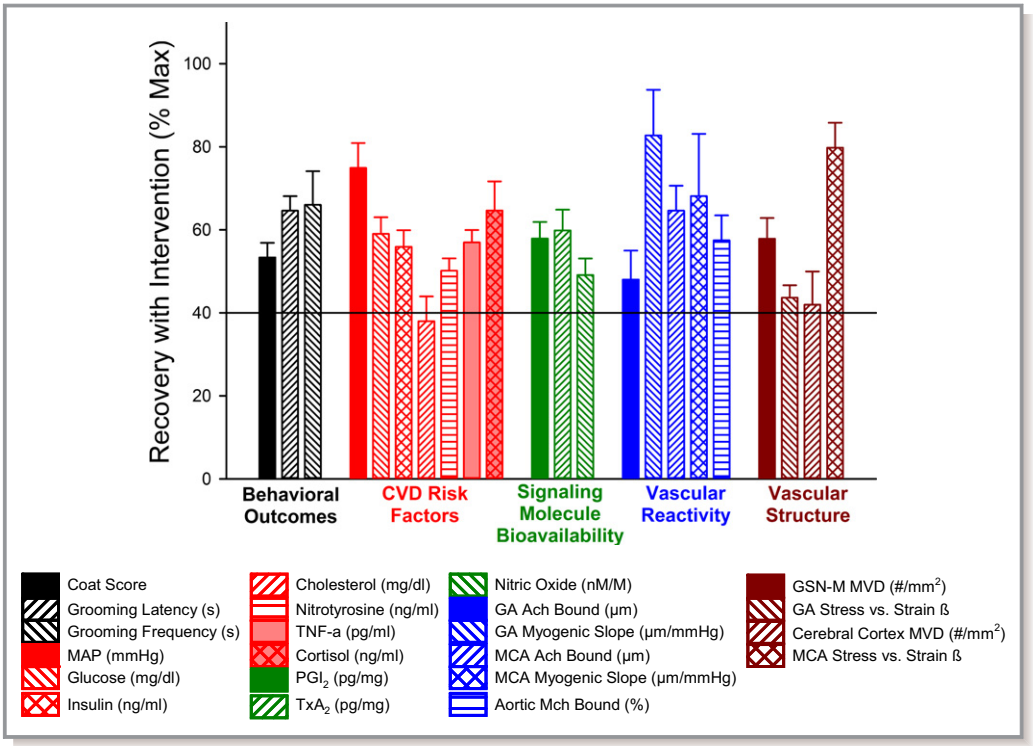

Figure 1. The effectiveness of long-term exercise from 7 weeks of age at maintaining specific indexes of behavioral outcomes, cardiovascular disease (CVD) risk factors, signaling molecule bioavailability, vascular reactivity, and vascular structure. Data (mean±SE) are summarized for obese Zucker rats in response to the long-term exercise protocol and are presented as the percentage of the maximum (Max) possible recovery in the specific parameter as a result of the intervention (Equation 6; please see text for details). Ach indicates acetylcholine; GA, gracilis arteriole; GSN-M, gastrocnemius muscle; MAP, mean arterial pressure; MCA, middle cerebral artery; Mch, methacholine; MVD, microvessel density;PGI_2, prostacyclin; TNF-α, tumor necrosis factor-α; and TxA_2, thromboxane A_2.

1. *Highest responders:* LZR aged control group (n=8 total observations).
2. *High responders:* exercise, antidyslipidemia (atorvastatin), antioxidant (TEMPOL), and anti-inflammatory (pentoxifylline) (n=32 total observations).
3. *Moderate responders:* antidyslipidemia (gemfibrozil), antihypertensive (captopril), antidiabetic (metformin), and antidiabetic (rosiglitazone) (n=32 total observations).
4. *Low responders:* OZR time control group and antihypertensive (hydralazine) (n=16 total observations).

Although there is heterogeneity in the size of these 4 groups, they are statistically defined on the basis of within-group homogeneity. Reassigning treatment groups to different clusters to "even out" the size of each cluster would introduce within-group heterogeneity and compromise the next analytic step. In particular, LZR control animals consistently and uniformly clustered to their own unique group. Finally, animals treated with either rosiglitazone or metformin, mechanistically different drugs to treat insulin resistance, clustered to the same behavioral outcome group, whereas animals treated with mechanistically different but target-identical drugs for hypertension (captopril or hydralazine) or cholesterol (atorvastatin or gemfibrozil) clustered to different behavioral outcome groups.

Step 2: factor analysis to identify latent vascular constructs. The vascular outcomes from each animal were described by a series of 14 distinct variables (the variables described in the Vascular Outcomes: Function and Reactivity, Vascular Outcomes: Structure, and Integrated Vascular Outcomes: Skeletal Muscle Blood Perfusion sections, previously described, and as reported in Tables 1 through 6). Collectively, these variables were both too numerous and too correlated to consider simultaneously in multivariable analyses. Thus, factor analysis was conducted to identify the latent constructs underlying these variables, and so reduce the total variable number into a fewer number of constructed factors. For this analysis, animals from all 11 treatment groups were included simultaneously (n=88 total observations). Factors were extracted using principal axis factoring and the Bartlett method, with a minimum accepted eigenvalue of 1.0. To account for correlation between factors, oblique rotation via the Promax method with Kaiser normalization was used.

Table 1. Characteristics of the Aged Control Group (Untreated LZRs and OZRs at 7W and 17W)

Characteristics	LZRs 7W	LZRs 17W	OZRs 7W	OZRs 17W
Behavioral outcomes				
Coat score	0.23±0.03	0.41±0.02*	0.51±0.05*	4.86±0.3*†‡
Grooming latency after sucrose spray, s	5.9±0.4	5.4±0.4	6.4±0.5	32.6±1.5*†‡
Grooming frequency after sucrose spray, s	18.1±1.0	18.6±1.1	16.4±0.9	5.8±0.5*†‡
CVD risk factors				
MAP, mm Hg	100±3	101±2	99±4	140±4*†‡
Glucose, mg/dL	91±3	97±4	104±3*	161±5*†‡
Insulin, ng/mL	1.1±0.1	1.2±0.1	3.7±0.3*	9.6±0.5*†‡
Cholesterol, mg/dL	82.1±2.9	81.9±3.8	92.9±3.9	134.3±4.2*†‡
Nitrotyrosine, ng/mL	11.5±0.9	13.1±1.5	12.5±1.0	58.0±2.5*†‡
TNF-α, pg/mL	1.5±0.2	1.6±0.3	2.4±0.2*	11.5±0.6*†‡
Cortisol, ng/mL	22.4±1.1	29.9±1.2*	37.1±2.9*	55.6±2.2*†‡
Signaling molecule bioavailability				
Prostacyclin, pg/mg	139.7±2.9	147.3±2.5	102.8±3.7*	22.9±1.5*†‡
TxA_2, pg/mg	34.8±3	51.9±2.8*	50.0±3.0*	138.8±2.9*†‡
NO, nmol/L/mol/L	52.1±2.1	57.1±1.8	51.4±1.3	15.3±1.5*†‡
Vascular outcomes: function and reactivity				
GA acetylcholine bound, μm	26.3±1.0	29.1±2.1	21.3±1.4	13.5±1.1*†‡
GA myogenic slope, μm/mm Hg	0.02±0.01	0.00±0.02	0.00±0.01	−0.14±0.02*†‡
GA norepinephrine bound, μm	−44.8±3	−45.4±2.5	−43.4±2.4	−55.9±3.4*†‡
MCA acetylcholine bound, μm	25.0±1.2	28.1±0.9	26.0±0.8	14.0±0.8*†‡
MCA myogenic slope, μm/mm Hg	−0.10±0.02	−0.12±0.02	−0.15±0.04	−0.30±0.05*†‡
MCA serotonin bound, μm	−30.5±2.2	−28.1±1.5	−26.3±1.3	−36.8±1.5*†‡
Aortic methacholine bound, %	91.5±1.6	92.6±1.8	88.5±1.9	65.0±2.4*†‡
Aortic norepinephrine bound, %	76.7±1.5	74.3±2.0	76.0±1.5	92.1±1.8*†‡
Vascular outcomes: structure				
GSN-M MVD, no./mm^2	768±6.4	771±10.4	758±8.6	643±11.8*†‡
GA stress vs strain β	3.14±0.13	3.44±0.09	3.48±0.16	6.64±0.25*†‡
Cerebral cortex MVD, no./mm^2	312±5.0	316±5.5	313±4.0	249±6.1*†‡
MCA stress vs strain β	1.60±0.05	1.80±0.04	1.82±0.06	2.98±0.15*†‡
Integrated vascular outcomes: skeletal muscle blood perfusion				
GSN-M resting blood flow, mL/100 g per minute	13.6±0.6	13.5±0.3	12.8±0.4	9.3±0.5*†‡
GSN-M hyperemia (3 Hz), mL/100 g per minute	63.6±3.2	67.8±2.1	62.5±3.0	50.4±1.3*†‡

Each animal group (column) consists of n=8 observations. 7W indicates 7 weeks old; 17W, 17 weeks old; CVD, cardiovascular disease; GA, gracilis arteriole; GSN-M, gastrocnemius muscle; LZR, lean Zucker rat; MAP, mean arterial pressure; MCA, middle cerebral artery; MVD, microvessel density; OZR, obese Zucker rat; TNF-α, tumor necrosis factor-α; and TxA_2, thromboxane A_2.

*Indicates statistical significance at $P<0.05$ vs LZR at 7W.

†Indicates statistical significance at $P<0.05$ vs OZR at 7W.

‡Indicates statistical significance at $P<0.05$ vs LZR at 17W.

Two factors were extracted after 3 iterations. The Kaiser-Meyer-Olkin Measure of Sampling Adequacy was 0.926 and the Bartlett's Test for Sphericity was statistically significant ($P<0.0001$). After extraction, the first factor explained 48.8% of the variance, and the second factor explained 4.7% of the variance (overall, 53.4% of the total variance explained). Additional details from this statistical analysis are reported in Tables S4 through S6. The 2 vascular factors were defined, on the basis of factor loading, as follows:

1. *Vascular Factor 1:* MCA acetylcholine bound, GA acetylcholine bound, GSN-M resting flow, GSN-M hyperemia, cerebral cortex MVD, and aorta norepinephrine bound.
2. *Vascular Factor 2:* MCA myogenic slope, GA myogenic slope, MCA stress versus strain slope, GA stress versus strain slope, skeletal muscle MVD, aorta methacholine bound, GA norepinephrine bound, and MCA serotonin bound.

The scores for both Vascular Factor 1 and Vascular Factor 2 were retained and used as independent (predictor) variables in the subsequent discriminant analysis.

Step 3: differentiating between the behaviorally based outcome groups (from cluster analysis) using discriminant analysis. We performed linear discriminant analysis to interrogate potential mechanistic links between behavioral impairments/depressive symptoms, vascular outcomes, biomarker expression profiling, and CVD-RFs. For this analysis, animals from all 11 treatment groups were included simultaneously (n=88 total observations). The 4 behaviorally based outcome groups defined during cluster analysis (previously described) were the grouping (dependent) variables, and the continuous predictive (independent) variables included in the analysis were the biomarkers for Signaling Molecule Bioavailability (NO bioavailability, prostacyclin, and TxA_2), biomarkers for CVD Risk Factors (nitrotyrosine, cortisol, and TNF-α), and the 2 vascular factor scores generated, as previously described (Vascular Factors 1 and 2).

Three canonical discriminant functions were generated, all of which were statistically significant ($P<0.001$). However, because the third function explained <1% of the total variance, it was not considered further. The first discriminant function explained 96.5% of the variance, with a canonical correlation coefficient of 0.981. The second discriminant function explained 2.8% of the variance, with a canonical correlation coefficient of 0.651. For tests of equality of group means (Wilk's λ), all independent variables were statistically significant ($P<0.0001$ for all), suggesting that all variables were important discriminators. The overall cross-validated classification accuracy was 98.9%. Additional details from this statistical analysis are reported in Tables S7 through S11.

Statistical analyses were performed using SPSS (IBM Analytics, Armonk, NY). Graphing was performed using SigmaPlot (Systat Software, Inc, San Jose, CA).

Results

Data describing the behavioral outcomes, CVD-RFs, signaling molecule bioavailability, and vascular outcomes of the aged control group are summarized in Table 1. These results, of 7W versus 17W OZRs and LZRs under untreated conditions, represent the effects of untreated aging on LZRs and OZRs. There were minimal differences between LZR at 7W and 17W (only coat score, cortisol, and TxA_2 were worse at 17W versus 7W). Furthermore, there were also relatively few differences between LZRs and OZRs at 7W of age (coat score, glucose, insulin, TNF-α, cortisol, prostacyclin, and TxA_2 were all worse in OZRs versus LZRs at 7W), although this did not translate into any alteration in vascular outcomes. In contrast, by 17W of age, OZRs had manifested the full complement of the metabolic syndrome and demonstrated striking changes to behavioral responses commensurate with elevated depressive symptoms. In fact, by 17W, the OZRs were statistically significantly worse than all 3 other animal groups (LZRs at 7W, LZRs at 17W, and OZRs at 7W) on all measured parameters, including all behavioral outcomes, CVD-RFs, signaling molecule bioavailability, and all vascular outcomes. Of particular note, the deterioration of behavioral status in the OZRs, indicative of the onset of depressive symptoms, occurred in the absence of any intervention or environmental stressing protocol (ie, the onset of depressive symptoms was spontaneous, occurring simultaneously with the onset of the metabolic syndrome and vasculopathy).

Impact of Treatment Protocols on Measured Parameters: Univariate Analysis

Results describing the impact of long-term treadmill exercise in OZRs are summarized in Table 2. In OZRs, long-term exercise from 7W to 17W had multifaceted significant impacts in reducing markers of CVD risk and in improving most indexes of both behavioral and vascular outcomes. These effects are underscored in Figure 1, which presents the effectiveness of exercise (Equation 6) in recovering parameters back to that in control LZRs. As shown in Figure 1, all parameters in OZRs treated with long-term exercise were recovered by at least 40%, with most parameters recovered by 50%, including all 3 behavioral outcome parameters.

In Table 3, results summarizing the impact of long-term treatment of OZRs from 7W to 17W with 2 mechanistically different antihypertensive agents, captopril and hydralazine, are presented. Although both captopril and hydralazine were effective at reducing hypertension (versus OZR control), hydralazine affected only 2 other measured parameters (GSN-M MVD and MCA stress strain β, both parameters of vascular structure outcomes). In contrast, compared with OZR control animals, captopril-treated animals had improved indexes of metabolic syndrome, including multiple CVD-RFs and signaling molecule

Table 2. Characteristics of the Exercise Group (Long-Term Exercise-Treated OZRs) and Untreated (Sedentary) Within-Group LZR and OZR Controls at 17W

	Within-Group Control (Sedentary)		Treated (Exercise)
Characteristics	LZRs	OZRs	OZRs
Behavioral outcomes			
Coat score	0.58±0.02	5.11±0.5*	2.49±0.6*†
Grooming latency after sucrose spray, s	6.1±0.5	29.8±2.2*	14.4±2.5*†
Grooming frequency after sucrose spray, s	19.4±1.4	7.4±2.0*	14.2±1.8*
CVD risk factors			
MAP, mm Hg	101±2	145±5*	118±4*†
Glucose, mg/dL	91±5	168±7*	122±7*†
Insulin, ng/mL	1.2±0.3	8.8±0.6*	4.8±0.5*†
Cholesterol, mg/dL	80±4	138±6*	115±6*†
Nitrotyrosine, ng/mL	13±2	55±5*	36±5*†
TNF-α, pg/mL	1.4±0.4	10.5±0.6*	5.9±0.5*†
Cortisol, ng/mL	30±3	58±5*	39±5†
Signaling molecule bioavailability			
Prostacyclin, pg/mg	140.1±4.0	28.9±4.0*	94.9±4.8*†
TxA_2, pg/mg	47.6±4.5	129.8±4.8*	86.8±5.1*†
NO, nmol/L/mol/L	50.8±3.8	19.7±2.5*	35.8±3.2*†
Vascular outcomes: function and reactivity			
GA acetylcholine bound, μm	28.4±2.0	14.0±1.4*	21.1±1.9*†
GA myogenic slope, μm/mm Hg	0.00±0.03	−0.14±0.03*	−0.03±0.02*†
GA norepinephrine bound, μm	−44.9±2.4	−56.2±2.8*	−46.3±2.8*†
MCA acetylcholine bound, μm	27.8±1.4	12.7±1.8*	23.1±2.8*†
MCA myogenic slope, μm/mm Hg	−0.16±0.02	−0.29±0.04*	−0.18±0.04*†
MCA serotonin bound, μm	−29.4±1.9	−33.8±2.0	−29.6±2.1*†
Aortic methacholine bound, %	94.2±2.4	61.5±2.5*	80.9±2.9*†
Aortic norepinephrine bound, %	71.9±2.0	90.9±2.1*	79.5±2.4*†
Vascular outcomes: structure			
GSN-M MVD, no./mm^2	748±12	626±16*	718±11*†
GA stress vs strain β	3.58±0.11	6.28±0.32*	5.20±0.28*†
Cerebral cortex MVD, no./mm^2	324±12	258±14*	280±12*†
MCA stress vs strain β	2.02±0.08	3.42±0.29*	2.24±0.35†
Integrated vascular outcomes: skeletal muscle blood perfusion			
GSN-M resting blood flow, mL/100 g per minute	12.4±0.3	9.4±0.4*	11.0±0.5*†
GSN-M hyperemia (3 Hz), mL/100 g per minute	66.4±3.8	48.9±2.3*	60.1±2.8*†

Each animal group (column) consists of n=8 observations. 17W indicates 17 weeks old; CVD, cardiovascular disease; GA, gracilis arteriole; GSN-M, gastrocnemius muscle; LZR, lean Zucker rat; MAP, mean arterial pressure; MCA, middle cerebral artery; MVD, microvessel density; OZR, obese Zucker rat; TNF-α, tumor necrosis factor-α; and TxA_2, thromboxane A_2.
*Indicates statistical significance at $P<0.05$ vs LZR untreated (sedentary) within-group control.
†Indicates statistical significance at $P<0.05$ vs OZR untreated (sedentary) within-group control.

bioavailability, as well as vascular function and reactivity, structural, and integrated perfusion outcomes. In addition, captopril-treated animals also showed improved markers of depressive symptoms (grooming latency and frequency). The broad differences between captopril and hydralazine are underscored in Figure 2, which summarizes the

Table 3. Characteristics of the Antihypertensive Treatment Group (Long-Term Pharmacologically Treated OZRs) and Untreated Within-Group Control LZRs and OZRs at 17W

	Within-Group Control (Untreated)		Treated (OZRs)	
Characteristics	LZRs	OZRs	Captopril	Hydralazine
Behavioral outcomes				
Coat score	0.51±0.05	5.1±0.5*	4.4±0.3*	5.0±0.6*
Grooming latency after sucrose spray, s	6.1±0.5	30.8±3.1*	23.5±1.6*†	34.6±2.5*
Grooming frequency after sucrose spray, s	19.4±1.6	6.5±0.8*	10.4±0.8*†	5.6±0.9*
CVD risk factors				
MAP, mm Hg	101±4	139±5*	107±5†	104±6†
Glucose, mg/dL	91±5	155±10*	143±7*	167±9*
Insulin, ng/mL	1.4±0.5	8.4±0.6*	6.6±0.5*†	9.5±0.7*
Cholesterol, mg/dL	79±5	141±8*	138±6*	136±6*
Nitrotyrosine, ng/mL	15±2	55±6*	35±5*†	47±8*
TNF-α, pg/mL	1.4±0.4	10.4±0.8*	8.2±0.6*†	10.8±0.8*
Cortisol, ng/mL	31±2	58±4*	45±4*†	54±6*
Signaling molecule bioavailability				
Prostacyclin, pg/mg	135±7	41±7*	46±6*	26±5*
TxA_2, pg/mg	44±6	129±7*	93±7*†	140±8*
NO, nmol/L/mol/L	53±4	18±4*	37±5*†	20±5*
Vascular outcomes: function and reactivity				
GA acetylcholine bound, μm	26.5±3.1	15.5±1.8*	22.1±2.4†	15.8±2.1*
GA myogenic slope, μm/mm Hg	0.01±0.01	−0.11±0.04*	−0.06±0.02*	−0.07±0.02*
GA norepinephrine bound, μm	−46±4	−57±6	−44±4†	−53±5
MCA acetylcholine bound, μm	27.1±2.2	16.0±2.8*	23.5±2.8†	17.3±2.4*
MCA myogenic slope, μm/mm Hg	−0.11±0.03	−0.28±0.05*	−0.20±0.04	−0.14±0.05
MCA serotonin bound, μm	−30.5±3.3	−40.1±3.4*	−25.4±2.5†	−35.5±2.7
Aortic methacholine bound, %	93.4±2.5	71.2±4.8*	86.9±4.4†	79.8±4.6*
Aortic norepinephrine bound, %	70.8±2.1	91.7±2.0*	85.1±1.9*†	89.2±2.2*
Vascular outcomes: structure				
GSN-M MVD, no./mm^2	756±14	636±14*	720±12*†	689±15*†
GA stress vs strain β	3.6±0.4	5.8±0.5*	4.9±0.4*†	4.7±0.6
Cerebral cortex MVD, no./mm^2	322±11	270±14*	295±12	266±6.1*
MCA stress vs strain β	2.4±0.4	4.1±0.5*	2.2±0.4†	2.0±0.5†
Integrated vascular outcomes: skeletal muscle blood perfusion				
GSN-M resting blood flow, mL/100 g per minute	12.8±0.3	8.9±0.6*	10.5±0.5*†	10.0±0.5*
GSN-M hyperemia (3 Hz), mL/100 g per minute	71.5±4.1	51.8±4.4*	57.0±4.1*	52.8±4.3*

Each animal group (column) consists of n=8 observations. Antihypertensive pharmacologic agents: captopril (angiotensin-converting enzyme inhibitor) and hydralazine (systemic vasodilator). 17W indicates 17 weeks old; CVD, cardiovascular disease; GA, gracilis arteriole; GSN-M, gastrocnemius muscle; LZR, lean Zucker rat; MAP, mean arterial pressure; MCA, middle cerebral artery; MVD, microvessel density; OZR, obese Zucker rat; TNF-α, tumor necrosis factor-α; and TxA_2, thromboxane A_2.

*Indicates statistical significance at $P<0.05$ vs LZR untreated within-group control.

†Indicates statistical significance at $P<0.05$ vs OZR untreated within-group control.

effectiveness (Equation 6) of captopril and hydralazine (Figure 2A and 2B, respectively) to restore measured parameters back to that in control LZRs. Captopril recovered 16 of 22 parameters, including all 3 behavioral parameters to at least 40% of control, whereas hydralazine only recovered 6 of 22 parameters to within 40% of control.

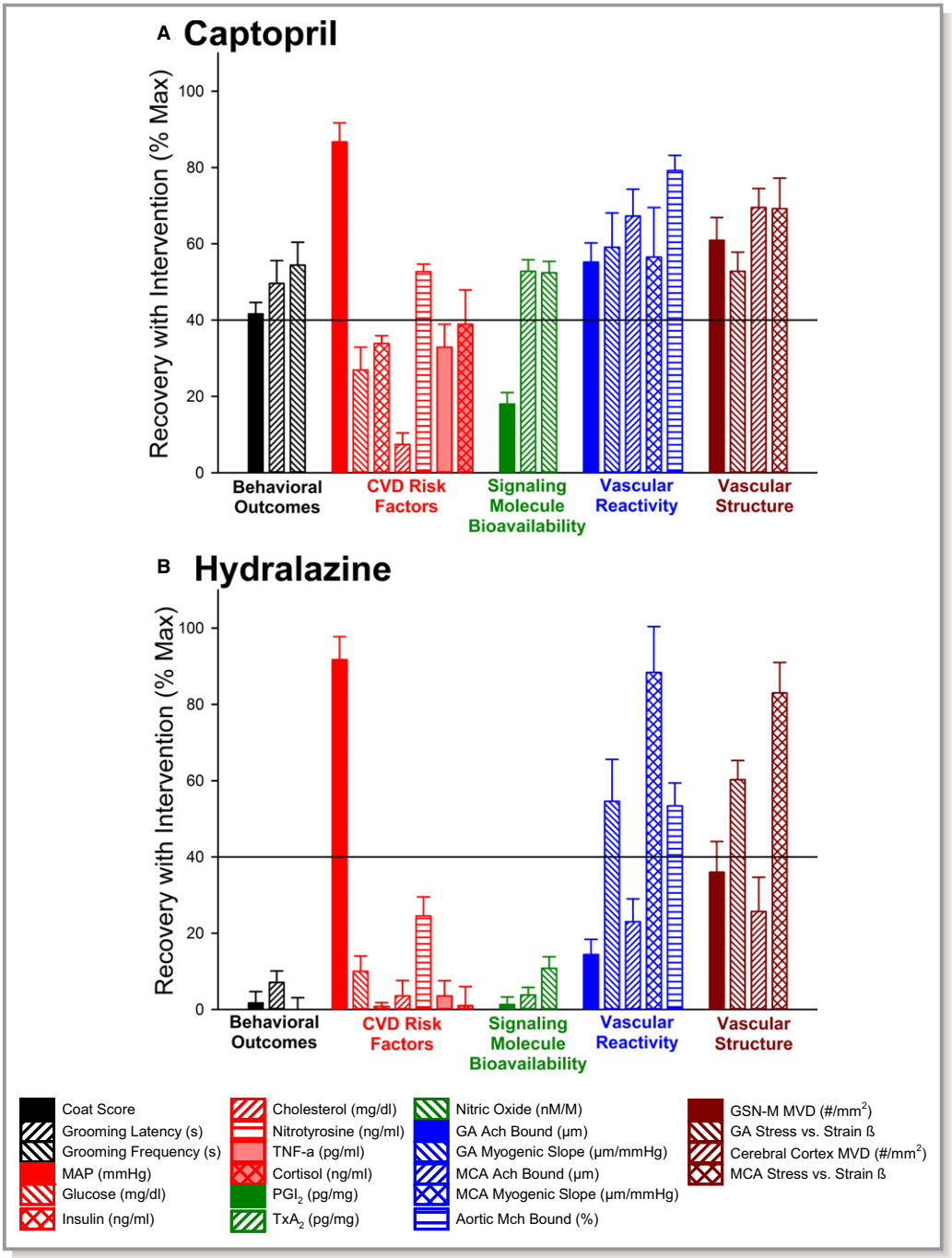

Figure 2. The effectiveness of long-term antihypertensive therapy from 7 weeks of age at maintaining specific indexes of behavioral outcomes, cardiovascular disease (CVD) risk factors, signaling molecule bioavailability, vascular reactivity, and vascular structure. Data (mean±SE) are summarized for obese Zucker rats in response to long-term treatment with either captopril (A) or hydralazine (B) and are presented as the percentage of the maximum (Max) possible recovery in the specific parameter as a result of the intervention (Equation 6; please see text for details). Ach indicates acetylcholine; GA, gracilis arteriole; GSN-M, gastrocnemius muscle; MAP, mean arterial pressure; MCA, middle cerebral artery; Mch, methacholine; MVD, microvessel density;PGI_2, prostacyclin; TNF-α, tumor necrosis factor-α; and TxA_2, thromboxane A_2.

Results summarizing the impact of long-term treatment of OZRs from 7W to 17W with mechanistically divergent antidiabetic agents, metformin and rosiglitazone, are presented in Table 4. As expected, both metformin and rosiglitazone were effective at reducing insulin resistance/hyperglycemia compared with OZR controls. In addition, both

Table 4. Characteristics of the Antidiabetic Treatment Group (Long-Term Pharmacologically Treated OZRs) and Untreated Within-Group Control LZRs and OZRs at 17W

	Within-Group Control (Untreated)		Treated (OZRs)	
Characteristics	LZRs	OZRs	Metformin	Rosiglitazone
Behavioral outcomes				
Coat score	0.4±0.1	5.1±0.6*	4.4±0.5*	4.2±0.5*
Grooming latency after sucrose spray, s	6.2±0.7	29.4±3.5*	27.1±2.5*	22.7±2.5*
Grooming frequency after sucrose spray, s	19.2±1.8	6.0±0.6*	9.3±0.7*†	11.8±0.7*†
CVD risk factors				
MAP, mm Hg	98±5	142±5*	138±6*	134±5*
Glucose, mg/dL	88±7	154±10*	98±7†	97±7†
Insulin, ng/mL	1.0±0.3	8.6±0.6*	3.9±0.7*†	3.6±0.6*†
Cholesterol, mg/dL	80±6	138±9*	147±7*	137±9*
Nitrotyrosine, ng/mL	14±4	51±6*	36±6*†	37±5*†
TNF-α, pg/mL	1.8±0.4	10.1±0.6*	6.0±0.7*†	5.9±0.6*†
Cortisol, ng/mL	28±3	59±4*	47±5*	41±5*†
Signaling molecule bioavailability				
Prostacyclin, pg/mg	137±9	40±5*	49±6*	63±6*†
TxA_2, pg/mg	48±5	129±6*	101±9*†	81±7*†
NO, nmol/L/mol/L	51±5	20±4*	38±5*†	36±5*†
Vascular outcomes: function and reactivity				
GA acetylcholine bound, μm	26.8±3.0	14.5±2.1*	22.4±2.5†	20.3±3.1†
GA myogenic slope, μm/mm Hg	−0.01±0.02	−0.11±0.03*	−0.12±0.02*	−0.11±0.03*
GA norepinephrine bound, μm	−46±6	−53±5	−54±4	−51±5
MCA acetylcholine bound, μm	25.9±2.5	12.0±1.9*	22.5±2.2†	24.0±2.0†
MCA myogenic slope, μm/mm Hg	−0.10±0.03	−0.27±0.05*	−0.23±0.04*	−0.21±0.05
MCA serotonin bound, μm	−33.4±2.9	−38.0±2.5	−30.0±3.5	−31.4±4.1
Aortic methacholine bound, %	94.1±2.6	65.0±5.4*	77.5±4.4*†	76.5±3.4*†
Aortic norepinephrine bound, %	72.4±1.9	92.0±2.2*	90.2±1.2*	84.5±2.4*†
Vascular outcomes: structure				
GSN-M MVD, no./mm^2	760±16	626±16*	661±12*†	673±14*†
GA stress vs strain β	3.5±0.4	6.2±0.5*	5.8±0.5*	5.4±0.4*
Cerebral cortex MVD, no./mm^2	320±11	250±12*	284±13*†	278±10*†
MCA stress vs strain β	2.2±0.3	3.4±0.3*	2.6±0.4	2.3±0.4†
Integrated vascular outcomes: skeletal muscle blood perfusion				
GSN-M resting blood flow, mL/100 g per minute	12.2±0.5	9.9±0.6*†	9.9±0.5*	11.0±0.4
GSN-M hyperemia (3 Hz), mL/100 g per minute	68.0±4.5	51.5±4.3*†	52.7±3.3*	54.7±3.5†

Each animal group (column) consists of n=8 observations. Antidiabetic pharmacologic agents: metformin (hepatic gluconeogenesis inhibitor) and rosiglitazone (insulin-sensitizing agent). 17W indicates 17 weeks old; CVD, cardiovascular disease; GA, gracilis arteriole; GSN-M, gastrocnemius muscle; LZR, lean Zucker rat; MAP, mean arterial pressure; MCA, middle cerebral artery; MVD, microvessel density; OZR, obese Zucker rat; TNF-α, tumor necrosis factor-α; and TxA_2, thromboxane A_2.

*Indicates statistical significance at $P<0.05$ vs LZR untreated within-group control.

†Indicates statistical significance at $P<0.05$ vs OZR untreated within-group control.

also had similar pleiotropic effects on CVD-RFs and both vascular structure and function outcome parameters. As shown in Figure 3, the effectiveness (Equation 6) of long-term treatment with either metformin (Figure 3A) or rosiglitazone (Figure 3B) on the measured parameters of behavioral status, CVD-RFs, vascular structure, and function outcomes is presented. Despite their mechanistic disparity, both metformin and rosiglitazone exhibited a good ability to

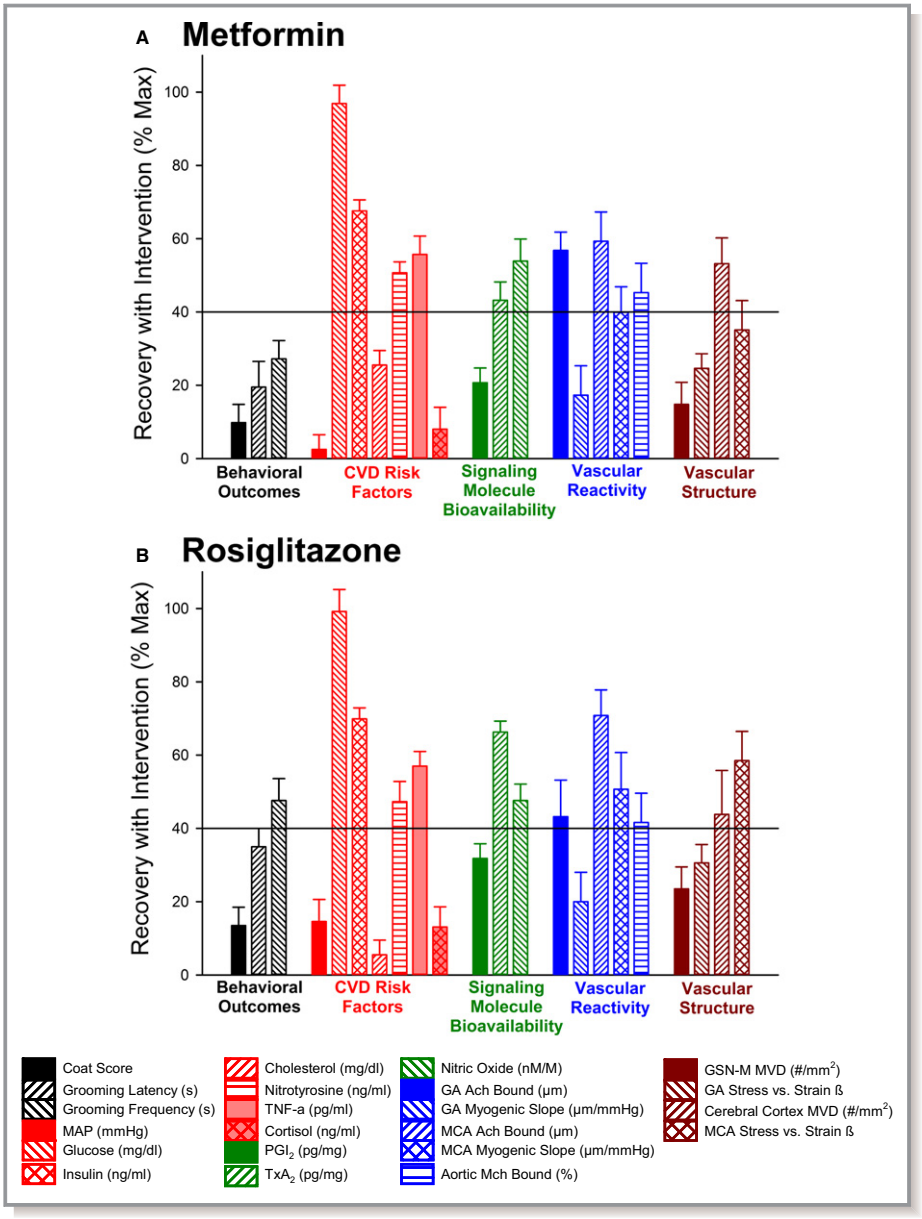

Figure 3. The effectiveness of long-term antidiabetic therapy from 7 weeks of age at maintaining specific indexes of behavioral outcomes, cardiovascular disease (CVD) risk factors, signaling molecule bioavailability, vascular reactivity, and vascular structure. Data (mean±SE) are summarized for obese Zucker rats in response to long-term treatment with either metformin (A) or rosiglitazone (B) and are presented as the percentage of the maximum (Max) possible recovery in the specific parameter as a result of the intervention (Equation 6; please see text for details). Ach indicates acetylcholine; GA, gracilis arteriole; GSN-M, gastrocnemius muscle; MAP, mean arterial pressure; MCA, middle cerebral artery; Mch, methacholine; MVD, microvessel density; PGI_2, prostacyclin; TNF-α, tumor necrosis factor-α; and TxA_2, thromboxane A_2.

substantially recover multiple CVD-RFs and vascular structure and function outcomes (for multiple outcomes, >50% recovery was observed). However, both metformin and rosiglitazone demonstrated only modest recovery in behavioral outcomes (all but one parameter achieved <35% recovery).

Table 5 presents data describing the impact of long-term treatment of OZRs from 7W to 17W with antidyslipidemia agents, atorvastatin or gemfibrozil. As expected, both gemfibrozil and atorvastatin significantly reduced plasma lipid levels compared with OZR controls. However, atorvastatin (an HMG Co-A reductase inhibitor) also significantly affected (improved) multiple other CVD-RFs, vascular structure and function outcomes, and behavioral outcomes, whereas gemfibrozil (a fibrate) had few pleiotropic effects.

Table 5. Characteristics of the Antidyslipidemia Treatment Group (Long-Term Pharmacologically Treated OZRs) and Untreated Within-Group Control LZRs and OZRs at 17W

	Within-Group Control (Untreated)		Treated (OZRs)	
Characteristics	LZRs	OZRs	Atorvastatin	Gemfibrozil
Behavioral outcomes				
Coat score	0.7±0.2	5.2±0.5*	2.7±0.5*†	4.1±0.5*†
Grooming latency after sucrose spray, s	4.9±1.1	29.4±3.5*	19.3±2.5*†	31.0±4.5*
Grooming frequency after sucrose spray, s	18.0±3.0	5.4±1.6*	12.0±2.7*†	6.7±2.6*
CVD risk factors				
MAP, mm Hg	99±5	142±5*	132±3*	136±5*
Glucose, mg/dL	92±6	148±8*	136±5*	155±9*
Insulin, ng/mL	1.3±0.2	8.6±0.6*	5.9±0.6*†	9.5±0.6*
Cholesterol, mg/dL	79±8	134±8*	98±11†	98±8†
Nitrotyrosine, ng/mL	16±3	49±5*	26±5†	51±6*
TNF-α, pg/mL	1.1±0.3	10.1±0.7*	11.5±0.6*†	9.5±0.7*
Cortisol, ng/mL	30±5	55±4*	42±5*	49±5*
Signaling molecule bioavailability				
Prostacyclin, pg/mg	129±12	42±5*	92±8*†	64±6*†
TxA_2, pg/mg	48±5	125±7*	94±9*†	107±6*†
NO, nmol/L/mol/L	51±5	19±3*	43±5†	18±4*
Vascular outcomes: function and reactivity				
GA acetylcholine bound, μm	27.4±2.5	14.1±2.8*	24.1±3.0*	16.1±2.2*
GA myogenic slope, μm/mm Hg	0.00±0.03	−0.12±0.03*	−0.07±0.02*	−0.13±0.03*
GA norepinephrine bound, μm	−48±4	−55±6	−46±5	−54±4
MCA acetylcholine bound, μm	26.2±2.7	15.0±2.4*	22.5±2.8†	18.1±1.8*
MCA myogenic slope, μm/mm Hg	−0.14±0.03	−0.31±0.05*	−0.21±0.03	−0.25±0.04*
MCA serotonin bound, μm	−28±4	−34±5	−27±4	−35±4
Aortic methacholine bound, %	95.6±1.8	61.0±4.8*	82.3±2.4*†	71.4±3.1*
Aortic norepinephrine bound, %	70.4±2.0	92.2±2.3*	82.0±1.8*†	88.5±2.1*
Vascular outcomes: structure				
GSN-M MVD, no./mm^2	754±15	640±15*	709±12*†	647±13*
GA stress vs strain β	3.6±0.5	6.1±0.6*	5.2±0.5*	6.0±0.4*
Cerebral cortex MVD, no./mm^2	324±14	252±14*	269±6.1*†	260±12*
MCA stress vs strain β	2.1±0.4	3.4±0.5*	2.1±0.4†	2.7±0.5
Integrated vascular outcomes: skeletal muscle blood perfusion				
GSN-M resting blood flow, mL/100 g per minute	13.1±0.4	9.8±0.5*	10.3±0.5*	10.4±0.6*
GSN-M hyperemia (3 Hz), mL/100 g per minute	70.9±4.0	51.1±4.2*	58.6±3.9†	51.1±2.9*

Each animal group (column) consists of n=8 observations. Antidyslipidemia pharmacologic agents: atorvastatin (HMG Co-A reductase inhibitor) and gemfibrozil (peroxisome proliferator-activated receptor-α activator). 17W indicates 17 weeks old; CVD, cardiovascular disease; GA, gracilis arteriole; GSN-M, gastrocnemius muscle; LZR, lean Zucker rat; MAP, mean arterial pressure; MCA, middle cerebral artery; MVD, microvessel density; OZR, obese Zucker rat; TNF-α, tumor necrosis factor-α; and TxA_2, thromboxane A_2.

*Indicates statistical significance at $P<0.05$ vs LZR untreated within-group control.

†Indicates statistical significance at $P<0.05$ vs OZR untreated within-group control.

These broad differences between atorvastatin and gemfibrozil are highlighted in Figure 4A and 4B, respectively. Atorvastatin-treated animals achieved 50% recovery (Equation 6) on almost all measured parameters, whereas gemfibrozil-treated animals only achieved 50% recovery on 1 parameter (cholesterol).

The results describing the impact of long-term treatment of OZRs from 7W to 17W with the antioxidant TEMPOL or the

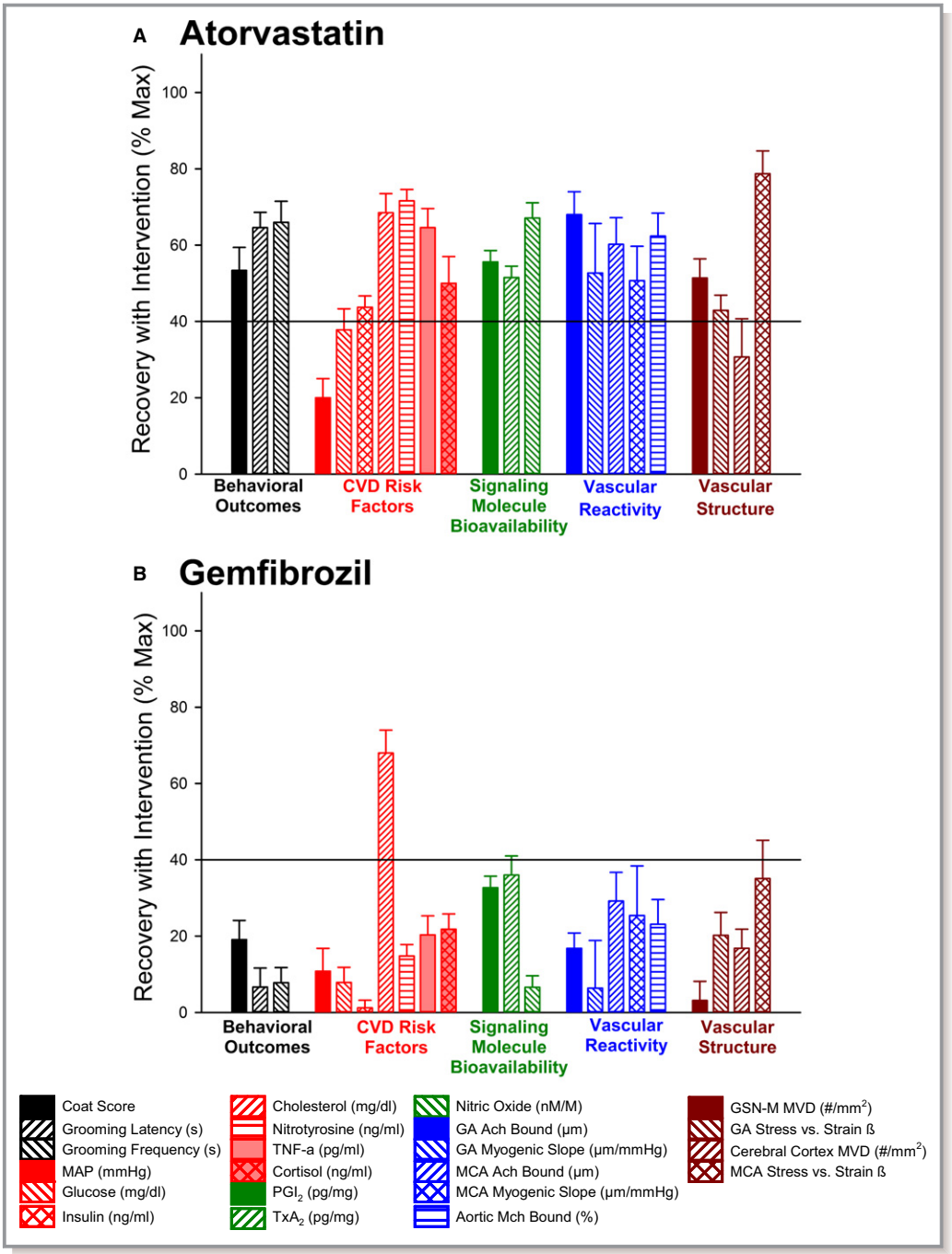

Figure 4. The effectiveness of long-term antidyslipidemic therapy from 7 weeks of age at maintaining specific indexes of behavioral outcomes, cardiovascular disease (CVD) risk factors, signaling molecule bioavailability, vascular reactivity, and vascular structure. Data (mean±SE) are summarized for obese Zucker rats in response to long-term treatment with either atorvastatin (A) or gemfibrozil (B) and are presented as the percentage of the maximum (Max) possible recovery in the specific parameter as a result of the intervention (Equation 6; please see text for details). Ach indicates acetylcholine; GA, gracilis arteriole; GSN-M, gastrocnemius muscle; MAP, mean arterial pressure; MCA, middle cerebral artery; Mch, methacholine; MVD, microvessel density; PGI_2, prostacyclin; TNF-α, tumor necrosis factor-α; and TxA_2, thromboxane A_2.

anti-inflammatory agent pentoxifylline are summarized in Table 6. Overall, the broad effect of the reduction in systemic chronic oxidant stress (TEMPOL) or in systemic chronic inflammation (pentoxifylline) on most measured parameters was similar. Both TEMPOL and pentoxifylline were comparable in their impacts on behavioral outcomes, vascular structure and function outcomes, as well as perfusion responses in the skeletal muscle. The equivalence in these 2 mechanistically

Table 6. Characteristics of the Antioxidant/Anti-Inflammatory Treatment Group (Long-Term Pharmacologically Treated OZRs) and Untreated Within-Group Control LZRs and OZRs at 17W

	Within-Group Control (Untreated)		Treated (OZRs)	
Characteristics	LZRs	OZRs	TEMPOL	Pentoxifylline
Behavioral outcomes				
Coat score	0.7±0.1	5.5±0.7*	3.0±0.4*†	3.6±0.5*†
Grooming latency after sucrose spray, s	6.1±0.6	28.0±4.1*	18.6±2.5*†	20.3±2.2*
Grooming frequency after sucrose spray, s	19.8±2.0	6.2±1.5*	12.8±1.8*†	12.3±0.6*†
CVD risk factors				
MAP, mm Hg	104±3	139±6*	112±5†	118±5*†
Glucose, mg/dL	93±5	145±10*	160±9*	137±9*
Insulin, ng/mL	1.3±0.2	8.9±0.7*	9.6±0.6*	7.8±0.6*
Cholesterol, mg/dL	85±8	128±9*	139±8*	137±9*
Nitrotyrosine, ng/mL	14±4	49±6*	18±4†	35±3*†
TNF-α, pg/mL	1.4±0.5	9.0±0.6*	6.1±0.7*†	2.5±0.6†
Cortisol, ng/mL	28±5	56±5*	31±4†	39±5†
Signaling molecule bioavailability				
Prostacyclin, pg/mg	141±8	49±6*	99±11*†	68±8*†
TxA_2, pg/mg	48±5	119±11*	66±9†	75±8*†
NO, nmol/L/mol/L	51±4	20±4*	41±5†	42±4†
Vascular outcomes: function and reactivity				
GA acetylcholine bound, μm	27.5±2.5	13.7±2.5*	21.6±3.2†	20.6±2.7*†
GA myogenic slope, μm/mm Hg	0.01±0.01	−0.09±0.02*	−0.04±0.02*	−0.07±0.02*
GA norepinephrine bound, μm	−47±5	−53±5	−46±5	−47±4†
MCA acetylcholine bound, μm	25.6±1.9	16.0±2.2*	23.8±2.6†	23.6±2.8†
MCA myogenic slope, μm/mm Hg	−0.09±0.02	−0.28±0.04*	−0.17±0.03*†	−0.21±0.04*
MCA serotonin bound, μm	−30±5	−36±4	−29±5	−30±5
Aortic methacholine bound, %	93.4±2.8	60.8±3.9*	87.6±4.1†	82.1±3.8*†
Aortic norepinephrine bound, %	70.8±1.9	91.1±2.1*	80.3±2.1*†	81.0±2.2*†
Vascular outcomes: structure				
GSN-M MVD, no./mm^2	752±14	626±14*	732±12†	711±14*††
GA stress vs strain β	3.5±0.4	5.8±0.5*	5.1±0.4*	5.1±0.5*
Cerebral cortex MVD, no./mm^2	322±12	264±11*	312±11†	304±11†
MCA stress vs strain β	1.9±0.4	3.6±0.5*	2.0±0.5†	2.4±0.5†
Integrated vascular outcomes: skeletal muscle blood perfusion				
GSN-M resting blood flow, mL/100 g per minute	12.4±0.5	10.2±0.4*	11.1±0.5	11.8±0.5†
GSN-M hyperemia (3 Hz), mL/100 g per minute	71.5±3.4	52.6±4.0*	60.1±3.9*†	58.5±3.3*

Each animal group (column) consists of n=8 observations. Pharmacologic agents: TEMPOL (antioxidant) and pentoxifylline (anti-inflammatory via TNF-α production inhibition). 17W indicates 17 weeks old; CVD, cardiovascular disease; GA, gracilis arteriole; GSN-M, gastrocnemius muscle; LZR, lean Zucker rat; MAP, mean arterial pressure; MCA, middle cerebral artery; MVD, microvessel density; OZR, obese Zucker rat; TNF-α, tumor necrosis factor-α; and TxA_2, thromboxane A_2.

*Indicates statistical significance at $P<0.05$ vs LZR untreated within-group control.

†Indicates statistical significance at $P<0.05$ vs OZR untreated within-group control.

different pharmacologic agents in recovering function (Equation 6) in the different measured parameters is underscored in Figure 5: most parameters for both TEMPOL (Figure 5A) and pentoxifylline (Figure 5B) achieved 50% recovery from control animals. Interesting, both TEMPOL and pentoxifylline had the least impact on traditional CVD-RFs.

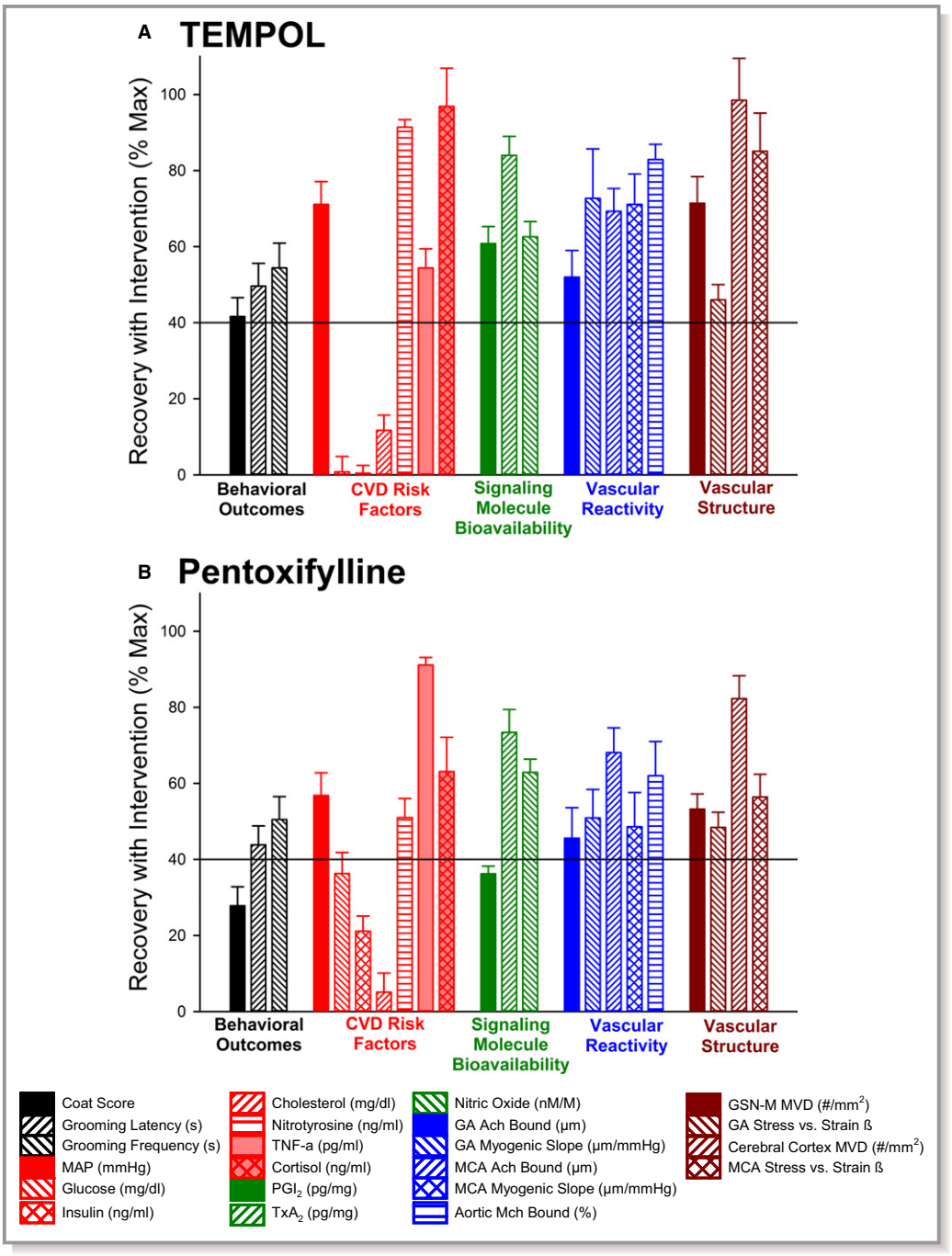

Figure 5. The effectiveness of long-term antioxidant or anti-inflammation therapy from 7 weeks of age at maintaining specific indexes of behavioral outcomes, cardiovascular disease (CVD) risk factors, signaling molecule bioavailability, vascular reactivity, and vascular structure. Data (mean±SE) are summarized for obese Zucker rats in response to long-term treatment with either TEMPOL (A) or pentoxifylline (B), and are presented as the percentage of the maximum (Max) possible recovery in the specific parameter as a result of the intervention (Equation 6; please see text for details). Ach indicates acetylcholine; GA, gracilis arteriole; GSN-M, gastrocnemius muscle; MAP, mean arterial pressure; MCA, middle cerebral artery; Mch, methacholine; MVD, microvessel density; PGI_2, prostacyclin; TNF-α, tumor necrosis factor-α; and TxA_2, thromboxane A_2.

Interrogating Mechanistic Links: Multistage Multivariable Analysis and Integrated Responses

Linear discriminant analysis was performed, as previously described, with Vascular Factors 1 and 2 (from factor analysis, previously described), the biomarkers for Signaling Molecule Bioavailability (NO bioavailability, prostacyclin, and TxA_2), and biomarkers for CVD Risk Factors (nitrotyrosine, cortisol, and TNF-α) as the independent variables to discriminate between the 4 behaviorally based outcome groups (from cluster

analysis, previously described). Using the standardized canonical discriminant function coefficients, the 2 discriminant functions are as follows:

$$F_1 \int (0.94 \times PGI_2) - (0.69 \times TNF\ \propto) - (0.42 \times \text{Cortisol}) + (0.41 \times \text{Vascular Factor 1}) + (0.24 \times \text{NO Bioavailability}) + (0.12 \times \text{Nitrotyrosine}) - (0.06 \times \text{Vascular Factor 2}) - (0.01 \times TxA_2) + \varepsilon$$

Function 1

$$F_2 \int (0.89 \times TxA_2) - (0.70 \times \text{Cortisol}) + (0.33 \times \text{Vascular Factor 2}) - (0.20 \times TNF\ \propto) + (0.16 \times PGI_2) - (0.11 \times \text{Vascular Factor 1}) - (0.06 \times \text{NO Bioavailability}) - (0.06 \times \text{Nitrotyrosine}) + \varepsilon$$

Function 2

Thus, differentiation between the 4 behaviorally based outcome groups along Function 1 ("*x* axis"), which accounted for 96.5% of the variance, was predominately determined by prostacyclin, TNF-α, cortisol, and Vascular Factor 1. Differentiation between the 4 groups along Function 2 was smaller, accounting for 2.8% of the variance, and was determined by TXA_2, cortisol, Vascular Factor 2, and TNF-α. The separation of the 4 behaviorally based outcome groups using the discriminant functions is presented graphically in Figure 6.

The relationships between the percentage recovery in the behavioral outcomes and GSN-M hyperemia for each of the treatment groups are presented in Figure 7. Percentage recovery for behavioral outcomes was calculated as the unweighted average of the recovery in coat score, grooming latency, and grooming frequency for each animal within the group. GSN-M hyperemia was selected because, of all the parameters measured in this study, it is the most integrated and functional response (the ability of an entire vascular bed to meet the workload and metabolic demands of a [skeletal] muscle). From this visualization of the ability of the interventions to simultaneously restore both behavioral outcomes and integrated systemic vascular outcomes, long-term exercise and treatment with atorvastatin, TEMPOL, or pentoxifylline were most effective at improving this relationship in OZRs.

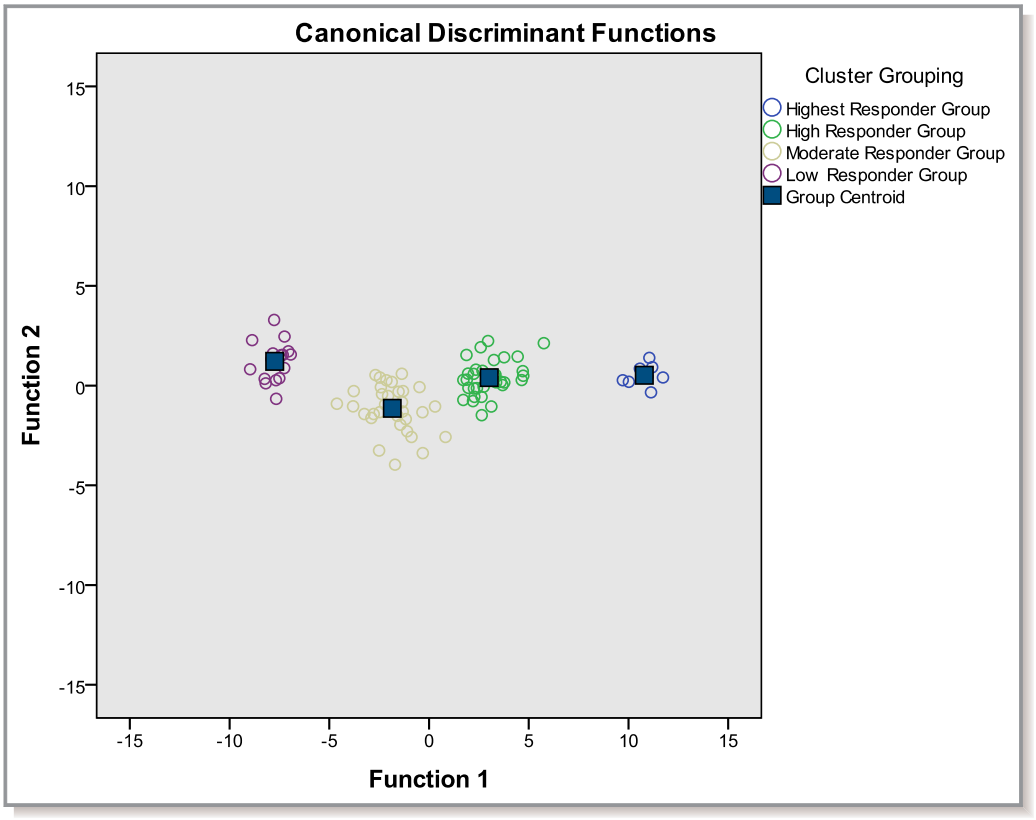

Figure 6. Canonical discriminant functions plot for the results of the discriminant analyses showing the plot of each discriminant function score for functions 1 and 2 (see Results section) for all obese Zucker rats in all treatment groups, and group centroids for each of the behavioral outcome groups defined by cluster analysis (see Methods section).

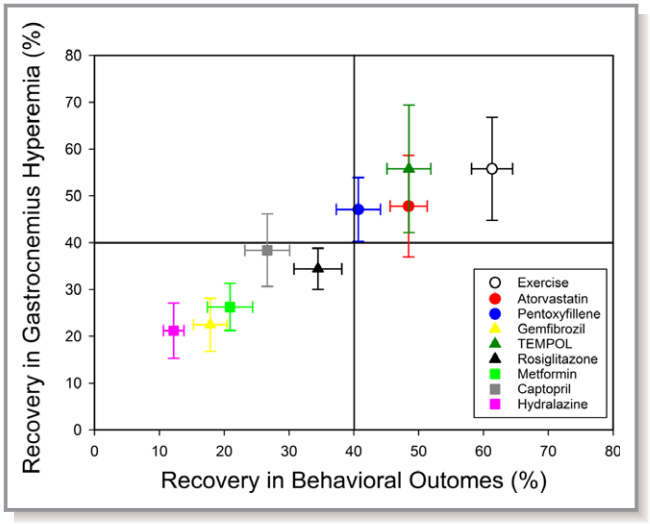

Figure 7. Plot of the simultaneous comparison of the percentage recovery in behavioral outcomes (coat score, grooming latency, and grooming frequency) and gastrocnemius hyperemia for each treatment group in the study. Results are presented as the average value(s) for all individual animals in a treatment group ±SE. In comparison to treatment groups in the lower left quadrant, animals in treatment groups in the upper right quadrant better maximized both behavioral outcomes and integrated systemic vascular function as a result of the intervention.

Discussion

The novel contribution of this study is the combination of the study design, with global (exercise) and single-target (pharmacologic) interventions, combined with multistage statistical modeling to provide insight into the complex mechanistic pathways between metabolic disease, CVD-RFs, vascular outcomes, and depressive symptoms. Observations from this study are, thus, particularly compelling and translationally relevant in light of observations from epidemiological and clinical research reporting a strong relationship between the prevalence and severity of CVD and the concurrent development of depressive symptoms.[17,19]

In previous studies, we have reported that, under conditions of chronically elevated CVD risk stemming from metabolic disease, OZRs spontaneously develop depressive symptoms[11,12]; these observations were again replicated in this study. In the OZRs, these depressive symptoms develop in parallel to a steadily decreasing level of physical activity (ie, increasing sedentary behavior) and a wide array of CVD-RFs that have been previously documented. These include alterations to biomarker profiles; endothelial function; vascular structure and reactivity in multiple organs, the brain, and skeletal muscle; and indexes of tissue/organ perfusion.[9,43] Consequently, the accurate identification of mechanistic links between metabolic disease, CVD-RFs and vascular outcomes, and depressive symptoms can be exceedingly difficult. Clearly, with these myriad alterations occurring in parallel in OZRs, there may be a cascade of impairments to vascular structure and function that predisposes physiologic systems to impaired function, with the aggregate output being a parallel development of both ischemic vascular disease and depressive symptoms.

A central result from the present study was the observed pleiotropic effects on behavioral outcomes from cardiovascular-targeted interventions. Although the general behavioral responses (coat status score and grooming responses) were strongly related to the age and severity of metabolic syndrome in control (untreated) LZRs and OZRs throughout the age ranges (7W–17W), significant divergence in the maintenance of the behavioral outcomes was observed as a result of the different long-term interventions. Using insights from the 3-stage statistical analysis, treatment with exercise was most effective in maintaining behavioral outcomes, followed by the 3 pharmacologic interventions of TEMPOL, pentoxifylline, and atorvastatin. All 4 of these interventions resulted in a recovery of behavioral outcomes of at least 40%. The 4 interventions, rosiglitazone, captopril, metformin, and gemfibrozil, achieved modest recovery in the behavioral outcomes (>15% but <40%), and animals treated with hydralazine were least able to maintain their behavioral outcomes. The ability of any of these 8 cardiovascular-targeted pharmacologic interventions to affect depressive symptoms clearly represents pleiotropic behavioral effects of these interventions and a novel and intriguing observation.

Mechanisms Underlying the Link Between Vascular Outcomes and Depressive Symptoms

Results from linear discriminant analysis indicate that the ability to maintain behavioral outcomes is contingent on the following: robust levels of vascular prostacyclin production, which is partially reflective of healthy endothelial function; reduced TNF-α and cortisol, which is indicative of reduced stress hormones and inflammation; and vascular function characteristics that are generally indicative of improved endothelial cell function (Vascular Function 1). Prostacyclin, TNF-α, cortisol, and endothelial function are also well recognized as strong predictors of, and parameters for, cardiovascular risk and disease. Thus, our findings are also consistent with recently published systematic reviews that all hypothesize that systematic immune function, hypothalamic-pituitary-adrenocortical axis, and endothelia function all represent likely mechanistic links between depression and CVD.[47–49] In our study, we are able to gain additional insight into the mechanistic underpinnings linking metabolic disease, CVD risk and function, and depressive symptoms by

examining the differential results observed between intervention groups.

We observed distinct, and disparate, patterns of results between the intervention groups in all measured domains (behavioral outcomes, CVD-RFs, signaling molecule bioavailability, vascular structure, and vascular function). The imposition of long-term exercise was successful at improving indexes of CVD risk, vascular outcomes, and depressive symptoms. Pharmacologic interventions targeting traditional CVD-RFs were effective in restoring the therapeutic target, but they were highly variable in addressing other (ie, off-target) vascular and/or behavioral outcomes. Clear separation between treatment groups was also observed in the aggregate conjoint comparison of behavioral outcomes and systemic cardiovascular function, as measured by the hyperemic response in the GSN-Ms. The hyperemic response is an integrated systemic response to an imposed physiologic challenge, with high translational relevance to clinical disease conditions in which ischemia is a fundamental contributor to poor outcomes. Exercise clearly optimizes both behavioral outcomes and integrated systemic cardiovascular function (Figure 7), followed by a group consisting of TEMPOL, atorvastatin, and pentoxifylline. Hydralazine had the lowest optimized effect on behavioral outcomes and integrated systemic cardiovascular function, with metformin and gemfibrozil achieving only slightly better integrated results. Captopril and rosiglitazone resulted in the "middle" level optimized results (ie, better than metformin and gemfibrozil, but not as good as TEMPOL, atorvastatin, or pentoxifylline).

Thus, it is intriguing to contemplate that the mechanistic link between metabolic disease, CVD-RFs and vascular outcomes, and depressive symptoms may not work through traditional CVD-RFs. Two of the most effective pharmacologic interventions, TEMPOL and pentoxifylline, had minimal effect on traditional CVD-RFs. Furthermore, different pharmacologic interventions with the same therapeutic target (a traditional CVD-RF) had different impacts on integrated systemic cardiovascular function (eg, atorvastatin versus gemfibrozil, captopril versus hydralazine, and rosiglitazone versus metformin). Rather, it is likely that the causal mechanisms linking metabolic disease, CVD-RFs and vascular outcomes, and depressive symptoms involve antioxidant and anti-inflammatory contributors that maintain endothelial function. The 4 interventions that were most effective in achieving optimized results in the aggregate conjoint comparison of behavioral outcomes and integrated systemic cardiovascular function (ie, exercise, TEMPOL, atorvastatin, and pentoxifylline) all share these common anti-inflammatory and antioxidant mechanisms, either directly (TEMPOL and pentoxifylline) or indirectly (exercise and atorvastatin). Exercise has well-known, global, physiologic effects that reduce both oxidant stress and inflammation, resulting in improved endothelial function,[50–53] and atorvastatin has recognized antioxidant and anti-inflammatory effects.[54] In contrast, our results suggest that hydralazine, a drug that is highly targeted to blood pressure reduction through its action as a smooth muscle dilator via hyperpolarization of the cell membrane,[55] was least effective in affecting behavioral outcomes and had negligible anti-inflammatory and antioxidant effects. The other pharmacological interventions in this study (captopril, rosiglitazone, metformin, and gemfibrozil) demonstrated middle effects on both behavioral outcomes as well as oxidant stress and inflammatory profiles. This is consistent with literature that suggests that the antioxidant and anti-inflammatory pleiotropic effects of these drugs are, while present, more modest in nature and may reflect an indirect impact on oxidant stress and inflammation that originates from reducing the severity of their therapeutic targets.[56,57]

The Role of Exercise

The broad-based beneficial impacts of long-term exercise on metabolic status, vascular health, and behavioral status warrant additional discussion. Although it has been clearly demonstrated that long-term exercise, or even long-term physical activity resulting in only modest elevations in metabolic demand, can have wide-ranging beneficial effects on antioxidant and anti-inflammatory defense,[58] there are also multiple other potential avenues through which exercise (or physical activity) can improve outcomes. In metabolic disease, systemic derangements negatively affect vascular structure at both the network and individual vessel level of resolution[59–62] and vascular reactivity to a wide array of stimuli that shift vascular tone towards elevated resistance[63,64]; there is an overall impairment to bulk blood flow[9] and the patterns of intramuscular perfusion distribution[43] and mass transport and exchange.[65–67] Long-term exercise has been repeatedly demonstrated to blunt the deterioration in all of these outcomes through an improvement in both the local vascular (eg, improved NO bioavailability) and systemic (eg, improved glycemic control) environments. Interestingly, although behavioral status and cardiovascular function were not the focus of the study, Martin-Cordero et al[68] demonstrated that long-term exercise training is an effective venue for reducing systemic corticosterone levels in OZRs in a manner that parallels the results of the present study. It seems likely that, given the widespread improvements to metabolic and vascular health experienced by OZRs subject to long-term exercise, the parallel improvements to behavioral status may reflect the widespread beneficial impacts of exercise, rather than any focused improvement to specific RFs or compromised mechanistic contributors. Results from this study may also provide mechanistic insight into findings from clinical

studies that have reported that exercise improves depressive symptoms in humans.[69]

Conclusions and Implications

Given an increasing emphasis and recognition of both CVD-RFs[16] and clinical depression[17,18] as diseases strongly associated with long-term elevations in oxidant stress and subacute inflammation, it is perhaps not surprising that these 4 interventions (exercise, TEMPOL, pentoxifylline, and atorvastatin) were most able to positively affect both vascular and behavioral outcomes. However, although these studies are provocative, they highlight the need to identify whether these relationships are also present in the cerebral circulation, which may have a much more direct impact on the behavioral responses. In addition, although exercise is a nonspecific intervention with effects on multiple physiologic systems, the other treatment groups in this study were singular pharmacologic interventions only which, while necessary for the purposes of this study design, limit insights into the effects of combination therapies often used in "real-world" clinical settings. Future studies should investigate these polytherapy effects as well as whether there are specific mechanistic links that, at a higher resolution, can be exploited with future interventional efforts. In addition, dosages for pharmacologic interventions were selected on the basis of the established clinically effective dose to treat that particular CVD-RF; future studies could explore whether pleiotropic behavioral effects are observed at subclinically effective doses. Finally, although a single animal model of the metabolic syndrome was used in this study, the OZR, future studies could explore whether the observations made herein are generalizable to other animal models of the metabolic syndrome or, more importantly, to human populations. Most notably, these results highlight the potential utility of a novel use of established therapeutics for CVD risk that may provide significant relief from the devastating impact of chronic depressive symptoms. It is anticipated that results from this study will provide translationally relevant insight into the primary prevention of both CVD and clinical depression.

Acknowledgments

We thank Milinda James for expert technical assistance.

Sources of Funding

This study was supported by the American Heart Association (IRG 14330015, PRE 16850005, and EIA 0740129N), the National Institutes of Health (RR 2865AR and R01 DK 64668), and the Natural Sciences and Engineering Research Council (R4218A03).

Disclosures

None.

References

1. Vassallo P, Driver SL, Stone NJ. Metabolic syndrome: an evolving clinical construct. *Prog Cardiovasc Dis*. 2016;59:172–177.
2. Tune JD, Goodwill AG, Sassoon DJ, Mather KJ. Cardiovascular consequences of metabolic syndrome. *Transl Res*. 2017;183:57–70.
3. Mameli C, Zuccotti GV, Carnovale C, Galli E, Nannini P, Cervia D, Perrotta C. An update on the assessment and management of metabolic syndrome, a growing medical emergency in paediatric populations. *Pharmacol Res*. 2017;119:99–117.
4. Alberti KG, Eckel RH, Grundy SM, Zimmet PZ, Cleeman JI, Donato KA, Fruchart JC, James WP, Loria CM, Smith SC Jr; International Diabetes Federation Task Force on Epidemiology and Prevention, National Heart, Lung, and Blood Institute, American Heart Association, World Heart Federation, International Atherosclerosis Society, and International Association for the Study of Obesity. Harmonizing the metabolic syndrome: a joint interim statement of the International Diabetes Federation Task Force on Epidemiology and Prevention; National Heart, Lung, and Blood Institute; American Heart Association; World Heart Federation; International Atherosclerosis Society; and International Association for the Study of Obesity. *Circulation*. 2009;120:1640–1645.
5. Global Burden of Metabolic Risk Factors for Chronic Diseases Collaboration. Cardiovascular disease, chronic kidney disease, and diabetes mortality burden of cardiometabolic risk factors from 1980 to 2010: a comparative risk assessment. *Lancet Diabetes Endocrinol*. 2014;2:634–647.
6. Shamseddeen H, Getty JZ, Hamdallah IN, Ali MR. Epidemiology and economic impact of obesity and type 2 diabetes. *Surg Clin North Am*. 2011;91:1163–1172, vii.
7. Trasande L, Elbel B. The economic burden placed on healthcare systems by childhood obesity. *Expert Rev Pharmacoecon Outcomes Res*. 2012;12:39–45.
8. Nilsson C, Raun K, Yan FF, Larsen MO, Tang-Christensen M. Laboratory animals as surrogate models of human obesity. *Acta Pharmacol Sin*. 2012;33:173–181.
9. Frisbee JC, Delp MD. Vascular function in the metabolic syndrome and the effects on skeletal muscle perfusion: lessons from the obese Zucker rat. *Essays Biochem*. 2006;42:145–161.
10. Guerre-Millo M. Regulation of ob gene and overexpression in obesity. *Biomed Pharmacother*. 1997;51:318–323.
11. Brooks SD, Stanley SC, Butcher JT, d'Audiffret A, Skaff PR, Chantler PD, Frisbee JC. Severity of behavioral impairments and vascular dysfunction with chronic stress/depressive symptoms is increased by metabolic syndrome. *Federations for the American Societies of Experimental Biology (FASEB) Annual Experimental Biology 2014 Meeting*San Diego, CA, April 26-30, 2014. *FASEB Journal*. 2014;28 (1 Suppl.):676.7. Available at: http://www.fasebj.org/doi/abs/10.1096/fasebj.29.1_supplement.789.4?legid=fasebj%3B29%2F1_Supplement%2F789.4&cited-by=yes.
12. Brooks SD, Stanley SC, Leon C, d'Audiffret A, Frisbee JC. Metabolic syndrome and chronic stress: convergent pathologies lead to severe vascular impairment. *Federations for the American Societies of Experimental Biology (FASEB) Annual Experimental Biology 2015 Meeting*Boston, MA, April 28-May 1, 2015. *FASEB Journal*. 2015;29 (1 Suppl.):789.4. Available at: http://www.fasebj.org/doi/abs/10.1096/fasebj.28.1_supplement.676.7.
13. Rebolledo-Solleiro D, Roldan-Roldan G, Diaz D, Velasco M, Larque C, Rico-Rosillo G, Vega-Robledo GB, Zambrano E, Hiriart M, Perez de la Mora M. Increased anxiety-like behavior is associated with the metabolic syndrome in non-stressed rats. *PLoS One*. 2017;12:e0176554.
14. Liu W, Liu J, Xia J, Xue X, Wang H, Qi Z, Ji L. Leptin receptor knockout-induced depression-like behaviors and attenuated antidepressant effects of exercise are associated with STAT3/SOCS3 signaling. *Brain Behav Immun*. 2017;61:297–305.
15. Pereira CD, Azevedo I, Monteiro R, Martins MJ. 11beta-Hydroxysteroid dehydrogenase type 1: relevance of its modulation in the pathophysiology of obesity, the metabolic syndrome and type 2 diabetes mellitus. *Diabetes Obes Metab*. 2012;14:869–881.
16. Bhatt H, Safford M, Glasser S. Coronary heart disease risk factors and outcomes in the twenty-first century: findings from the REasons for

Geographic and Racial Differences in Stroke (REGARDS) Study. *Curr Hypertens Rep*. 2015;17:541.

17. Goldstein BI, Carnethon MR, Matthews KA, McIntyre RS, Miller GE, Raghuveer G, Stoney CM, Wasiak H, McCrindle BW; American Heart Association Atherosclerosis, Hypertension and Obesity in Youth Committee of the Council on Cardiovascular Disease in the Young. Major depressive disorder and bipolar disorder predispose youth to accelerated atherosclerosis and early cardiovascular disease: a scientific statement from the American Heart Association. *Circulation*. 2015;132:965–986.
18. Dawood T, Barton DA, Lambert EA, Eikelis N, Lambert GW. Examining endothelial function and platelet reactivity in patients with depression before and after SSRI therapy. *Front Psychiatry*. 2016;7:18.
19. Hansen RA, Khodneva Y, Glasser SP, Qian J, Redmond N, Safford MM. Antidepressant medication use and its association with cardiovascular disease and all-cause mortality in the reasons for geographic and racial differences in stroke (REGARDS) study. *Ann Pharmacother*. 2016;50:253–261.
20. Stewart JC, Perkins AJ, Callahan CM. Effect of collaborative care for depression on risk of cardiovascular events: data from the IMPACT randomized controlled trial. *Psychosom Med*. 2014;76:29–37.
21. Overstreet DH. Modeling depression in animal models. *Methods Mol Biol*. 2012;829:125–144.
22. Willner P. Chronic mild stress (CMS) revisited: consistency and behavioural-neurobiological concordance in the effects of CMS. *Neuropsychobiology*. 2005;52:90–110.
23. Willner P. Validity, reliability and utility of the chronic mild stress model of depression: a 10-year review and evaluation. *Psychopharmacology*. 1997;134:319–329.
24. Willner P. The chronic mild stress (CMS) model of depression: history, evaluation and usage. *Neurobiol Stress*. 2017;6:78–93.
25. Willner P. Reliability of the chronic mild stress model of depression: a user survey. *Neurobiol Stress*. 2017;6:68–77.
26. Berton O, Nestler EJ. New approaches to antidepressant drug discovery: beyond monoamines. *Nat Rev Neurosci*. 2006;7:137–151.
27. d'Audiffret AC, Frisbee SJ, Stapleton PA, Goodwill AG, Isingrini E, Frisbee JC. Depressive behavior and vascular dysfunction: a link between clinical depression and vascular disease? *J Appl Physiol (1985)*. 2010;108:1041–1051.
28. Isingrini E, Camus V, Le Guisquet AM, Pingaud M, Devers S, Belzung C. Association between repeated unpredictable chronic mild stress (UCMS) procedures with a high fat diet: a model of fluoxetine resistance in mice. *PLoS One*. 2010;5:e10404.
29. Isingrini E, Surget A, Belzung C, Freslon JL, Frisbee J, O'Donnell J, Camus V, d'Audiffret A. Altered aortic vascular reactivity in the unpredictable chronic mild stress model of depression in mice: UCMS causes relaxation impairment to ACh. *Physiol Behav*. 2011;103:540–546.
30. Ortmann CF, Reus GZ, Ignacio ZM, Abelaira HM, Titus SE, de Carvalho P, Arent CO, Dos Santos MA, Matias BI, Martins MM, de Campos AM, Petronilho F, Teixeira LJ, Morais MO, Streck EL, Quevedo J, Reginatto FH. Enriched flavonoid fraction from cecropia pachystachya trecul leaves exerts antidepressant-like behavior and protects brain against oxidative stress in rats subjected to chronic mild stress. *Neurotox Res*. 2016;29:469–483.
31. Steckert AV, Dominguini D, Michels M, Abelaira HM, Tomaz DB, Sonai B, de Moura AB, Matos D, da Silva JBI, Reus GZ, Barichello T, Quevedo J, Dal-Pizzol F. The impact of chronic mild stress on long-term depressive behavior in rats which have survived sepsis. *J Psychiatr Res*. 2017;94:47–53.
32. Yalcin I, Belzung C, Surget A. Mouse strain differences in the unpredictable chronic mild stress: a four-antidepressant survey. *Behav Brain Res*. 2008;193:140–143.
33. Stanley SC, Brooks SD, Butcher JT, d'Audiffret AC, Frisbee SJ, Frisbee JC. Protective effect of sex on chronic stress- and depressive behavior-induced vascular dysfunction in BALB/cJ mice. *J Appl Physiol (1985)*. 2014;117:959–970.
34. Golbidi S, Frisbee JC, Laher I. Chronic stress impacts the cardiovascular system: animal models and clinical outcomes. *Am J Physiol Heart Circ Physiol*. 2015;308:H1476–H1498.
35. Nater UM, Skoluda N, Strahler J. Biomarkers of stress in behavioural medicine. *Curr Opin Psychiatry*. 2013;26:440–445.
36. Fabbri C, Hosak L, Mossner R, Giegling I, Mandelli L, Bellivier F, Claes S, Collier DA, Corrales A, Delisi LE, Gallo C, Gill M, Kennedy JL, Leboyer M, Lisoway A, Maier W, Marquez M, Massat I, Mors O, Muglia P, Nothen MM, O'Donovan MC, Ospina-Duque J, Propping P, Shi Y, St Clair D, Thibaut F, Cichon S, Mendlewicz J, Rujescu D, Serretti A. Consensus paper of the WFSBP Task Force on Genetics: genetics, epigenetics and gene expression markers of major depressive disorder and antidepressant response. *World J Biol Psychiatry*. 2017;18:5–28.
37. Butcher JT, Goodwill AG, Frisbee JC. The ex vivo isolated skeletal microvessel preparation for investigation of vascular reactivity. *J Vis Exp*. 2012;62:3674.
38. Kunert MP, Dwinell MR, Drenjancevic Peric I, Lombard JH. Sex-specific differences in chromosome-dependent regulation of vascular reactivity in female consomic rat strains from a SSxBN cross. *Am J Physiol Regul Integr Comp Physiol*. 2008;295:R516–R527.
39. Munzenmaier DH, Greene AS. Chronic angiotensin II AT1 receptor blockade increases cerebral cortical microvessel density. *Am J Physiol Heart Circ Physiol*. 2006;290:H512–H516.
40. Rieder MJ, O'Drobinak DM, Greene AS. A computerized method for determination of microvascular density. *Microvasc Res*. 1995;49:180–189.
41. Frisbee JC, Goodwill AG, Frisbee SJ, Butcher JT, Brock RW, Olfert IM, DeVallance ER, Chantler PD. Distinct temporal phases of microvascular rarefaction in skeletal muscle of obese Zucker rats. *Am J Physiol Heart Circ Physiol*. 2014;307:H1714–H1728.
42. Baumbach GL, Hajdu MA. Mechanics and composition of cerebral arterioles in renal and spontaneously hypertensive rats. *Hypertension*. 1993;21:816–826.
43. Frisbee JC, Butcher JT, Frisbee SJ, Olfert IM, Chantler PD, Tabone LE, d'Audiffret AC, Shrader CD, Goodwill AG, Stapleton PA, Brooks SD, Brock RW, Lombard JH. Increased peripheral vascular disease risk progressively constrains perfusion adaptability in the skeletal muscle microcirculation. *Am J Physiol Heart Circ Physiol*. 2016;310:H488–H504.
44. Liu Y, Fredricks KT, Roman RJ, Lombard JH. Response of resistance arteries to reduced PO2 and vasodilators during hypertension and elevated salt intake. *Am J Physiol*. 1997;273:H869–H877.
45. Catella F, Healy D, Lawson JA, FitzGerald GA. 11-Dehydrothromboxane B2: a quantitative index of thromboxane A2 formation in the human circulation. *Proc Natl Acad Sci U S A*. 1986;83:5861–5865.
46. Nies AS. Prostaglandins and the control of the circulation. *Clin Pharmacol Ther*. 1986;39:481–488.
47. Baune BT, Stuart M, Gilmour A, Wersching H, Heindel W, Arolt V, Berger K. The relationship between subtypes of depression and cardiovascular disease: a systematic review of biological models. *Transl Psychiatry*. 2012;2:e92.
48. Grippo AJ, Johnson AK. Stress, depression and cardiovascular dysregulation: a review of neurobiological mechanisms and the integration of research from preclinical disease models. *Stress*. 2009;12:1–21.
49. Joynt KE, Whellan DJ, O'Connor CM. Depression and cardiovascular disease: mechanisms of interaction. *Biol Psychiatry*. 2003;54:248–261.
50. Thijssen DH, Carter SE, Green DJ. Arterial structure and function in vascular ageing: are you as old as your arteries? *J Physiol*. 2016;594:2275–2284.
51. Golbidi S, Laher I. Exercise and the aging endothelium. *J Diabetes Res*. 2013;2013:789607.
52. Zhang H, Park Y, Wu J, Chen X, Lee S, Yang J, Dellsperger KC, Zhang C. Role of TNF-alpha in vascular dysfunction. *Clin Sci (Lond)*. 2009;116:219–230.
53. de Sousa CV, Sales MM, Rosa TS, Lewis JE, de Andrade RV, Simoes HG. The antioxidant effect of exercise: a systematic review and meta-analysis. *Sports Med*. 2017;47:277–293.
54. Profumo E, Buttari B, Saso L, Rigano R. Pleiotropic effects of statins in atherosclerotic disease: focus on the antioxidant activity of atorvastatin. *Curr Top Med Chem*. 2014;14:2542–2551.
55. Oates JA, Brown NJ. Antihypertensive agents and the drug therapy of hypertension. In: Hardman JG, Limbird LE, Gilman AG, eds. *Goodman & Gilman's The Pharmacological Basis of Therapeutics*. 10th ed. New York, NY: McGraw-Hill, Medical Publishing Division; 2001:871–900.
56. Kothari V, Galdo JA, Mathews ST. Hypoglycemic agents and potential anti-inflammatory activity. *J Inflamm Res*. 2016;9:27–38.
57. Omboni S, Malacco E, Napoli C, Modesti PA, Manolis A, Parati G, Agabiti-Rosei E, Borghi C. Efficacy of zofenopril vs. irbesartan in combination with a thiazide diuretic in hypertensive patients with multiple risk factors not controlled by a previous monotherapy: a review of the double-blind, randomized "Z" studies. *Adv Ther*. 2017;34:784–798.
58. Wagenmakers AJ, van Riel NA, Frenneaux MP, Stewart PM. Integration of the metabolic and cardiovascular effects of exercise. *Essays Biochem*. 2006;42:193–210.
59. Moore SM, Zhang H, Maeda N, Doerschuk CM, Faber JE. Cardiovascular risk factors cause premature rarefaction of the collateral circulation and greater ischemic tissue injury. *Angiogenesis*. 2015;18:265–281.
60. Brooks SD, DeVallance E, d'Audiffret AC, Frisbee SJ, Tabone LE, Shrader CD, Frisbee JC, Chantler PD. Metabolic syndrome impairs reactivity and wall mechanics of cerebral resistance arteries in obese Zucker rats. *Am J Physiol Heart Circ Physiol*. 2015;309:H1846–H1859.

61. Chantler PD, Shrader CD, Tabone LE, d'Audiffret AC, Huseynova K, Brooks SD, Branyan KW, Grogg KA, Frisbee JC. Cerebral cortical microvascular rarefaction in metabolic syndrome is dependent on insulin resistance and loss of nitric oxide bioavailability. *Microcirculation*. 2015;22:435–445.
62. Machado MV, Martins RL, Borges J, Antunes BR, Estato V, Vieira AB, Tibirica E. Exercise training reverses structural microvascular rarefaction and improves endothelium-dependent microvascular reactivity in rats with diabetes. *Metab Syndr Relat Disord*. 2016;14:298–304.
63. Sebai M, Lu S, Xiang L, Hester RL. Improved functional vasodilation in obese Zucker rats following exercise training. *Am J Physiol Heart Circ Physiol*. 2011;301:H1090–H1096.
64. Hodnett BL, Xiang L, Dearman JA, Carter CB, Hester RL. K(ATP)-mediated vasodilation is impaired in obese Zucker rats. *Microcirculation*. 2008;15:485–494.
65. Heinonen I, Koga S, Kalliokoski KK, Musch TI, Poole DC. Heterogeneity of muscle blood flow and metabolism: influence of exercise, aging, and disease states. *Exerc Sport Sci Rev*. 2015;43:117–124.
66. Poole DC, Musch TI. Muscle microcirculatory O(2) exchange in health and disease. *Adv Exp Med Biol*. 2010;662:301–307.
67. McClatchey PM, Frisbee JC, Reusch JEB. A conceptual framework for predicting and addressing the consequences of disease-related microvascular dysfunction. *Microcirculation*. 2017;24:e12359.
68. Martin-Cordero L, Garcia JJ, Hinchado MD, Ortega E. The interleukin-6 and noradrenaline mediated inflammation-stress feedback mechanism is dysregulated in metabolic syndrome: effect of exercise. *Cardiovasc Diabetol*. 2011;10:42.
69. Rimer J, Dwan K, Lawlor DA, Greig CA, McMurdo M, Morley W, Mead GE. Exercise for depression. *Cochrane Database Syst Rev*. 2012:7:CD004366.

SUPPLEMENTAL MATERIAL

Table S1. Correlation between cortisol, a biomarker associated with stress and depression, and behavioral outcomes (coat score, grooming latency, grooming frequency).

		COAT SCORE	GROOMING LATENCY (S)	GROOMING FREQUENCY (S)
CORTISOL (NG/ML)	PEARSON CORRELATION COEFFICIENT P-VALUE (2-TAILED)	0.655 p<0.0001	0.620 p<0.0001	-0.556 p<0.0001

S: seconds

Table S2. Supplementary statistical tables for cluster analysis: distances between final cluster centers.

CLUSTER	1	2	3	4
1		24.067	9.093	9.354
2	24.067		14.980	33.026
3	9.093	14.980		18.176
4	9.354	33.026	18.176	

Table S3. Supplementary statistical tables for cluster analysis: ANOVA.

	CLUSTER		ERROR			
	MEAN SQUARE	DF	MEAN SQUARE	DF	F STATISTIC	SIGNIFICANCE
COAT STATUS SCORE	37.160	3	0.749	84	49.583	0.000
GROOMING LATENCY	2305.184	3	8.596	84	268.178	0.000
GROOMING FREQUENCY	338.176	3	6.879	84	49.161	0.000

ANOVA: analysis of variance; DF: degrees of freedom

Table S4. Supplementary statistical tables for factor analysis: Kaiser-Meyer-Olkin and Bartlett's test.

KAISER-MEYER-OLKIN MEASURE OF SAMPLING ADEQUACY		0.926
BARTLETT'S TEST OF SPHERICITY	APPROXIMATE CHI-SQUARE	672.708
	DF	91
	SIGNIFICANCE	0.000

DF: degrees of freedom

Table S5. Supplementary statistical tables for factor analysis: Total variance explained.

FACTOR	INITIAL EIGENVALUES			EXTRACTION SUMS OF SQUARED LOADINGS			ROTATION SUMS OF SQUARED LOADINGS
	TOTAL	% OF VARIANCE	CUMULATIVE %	TOTAL	% OF VARIANCE	CUMULATIVE %	TOTAL
1	7.250	51.787	51.787	6.825	48.750	48.750	6.180
2	1.103	7.881	59.668	0.656	4.683	53.434	5.954
3	0.922	6.586	66.254				
4	0.803	5.735	71.989				
5	0.590	4.211	76.200				
6	0.557	3.978	80.178				
7	0.512	3.654	83.832				
8	0.488	3.486	87.318				
9	0.434	3.099	90.417				
10	0.340	2.432	92.849				
11	0.322	2.299	95.148				
12	0.270	1.927	97.076				
13	0.216	1.543	98.619				
14	0.193	1.381	100.000				

Table S6. Supplementary statistical tables for factor analysis: Factor correlation matrix.

FACTOR	1	2
1	1.000	0.756
2	0.756	1.000

Table S7. Supplementary statistical tables for discriminant analysis: Tests of equality for group Means.

	WILKS' LAMBDA	F STATISTIC	DF1	DF2	SIGNIFICANCE
NITROTYROSINE (NG/ML)	0.325	58.052	3	84	0.000
CORTISOL (NG/ML)	0.383	45.123	3	84	0.000
PGI_2 (PG/MG)	0.115	215.306	3	84	0.000
TXA_2 (PG/MG)	0.201	111.437	3	84	0.000
TNF-α (PG/ML)	0.275	73.925	3	84	0.000
NITRIC OXIDE (NM/M) BIOAVAILABILITY	0.288	69.376	3	84	0.000
VASCULAR FACTOR 1	0.255	81.953	3	84	0.000
VASCULAR FACTOR 2	0.535	24.340	3	84	0.000

DF: degrees of freedom; PGI_2: prostacyclin; TxA_2:thromboxane A_2

Table S8. Supplementary statistical tables for discriminant analysis: Box's test of equality of covariance matrices.

LOG DETERMINANTS		
CLUSTER GROUPING	RANK	LOG DETERMINANT
HIGHEST RESPONDER	--	--
HIGH RESPONDER	8	17.221
MODERATE RESPONDER	8	19.540
LOW RESPONDER	8	13.523
POOLED WITHIN-GROUPS	8	19.761

Table S9. Supplementary statistical tables for discriminant analysis: Test results.

BOX'S M	232.756
APPROX.	2.668
DF1	72
DF2	7571.954
SIGNIFICANCE	0.000

DF: degrees of freedom

Table S10. Supplementary statistical tables for discriminant analysis: Summary of canonical discriminant functions.

EIGENVALUES				
FUNCTION	EIGENVALUE	% OF VARIANCE	CUMULATIVE %	CANONICAL CORRELATION
1	25.715	96.5	96.5	0.981
2	0.736	2.8	99.2	0.651
3	0.208	0.8	100.0	0.415

Table S11. Supplementary statistical tables for discriminant analysis: Wilk's Lambda.

TEST OF FUNCTION(S)	WILKS' LAMBDA	CHI-SQUARE	DF	SIGNIFICANCE
1 THROUGH 3	0.018	326.063	24	0.000
2 THROUGH 3	0.477	59.959	14	0.000
3	0.828	15.299	6	0.018

DF: degrees of freedom